UNIVERSIDADE FEDERAL DO PARANÁ

EDSON LEONARDO DOS SANTOS

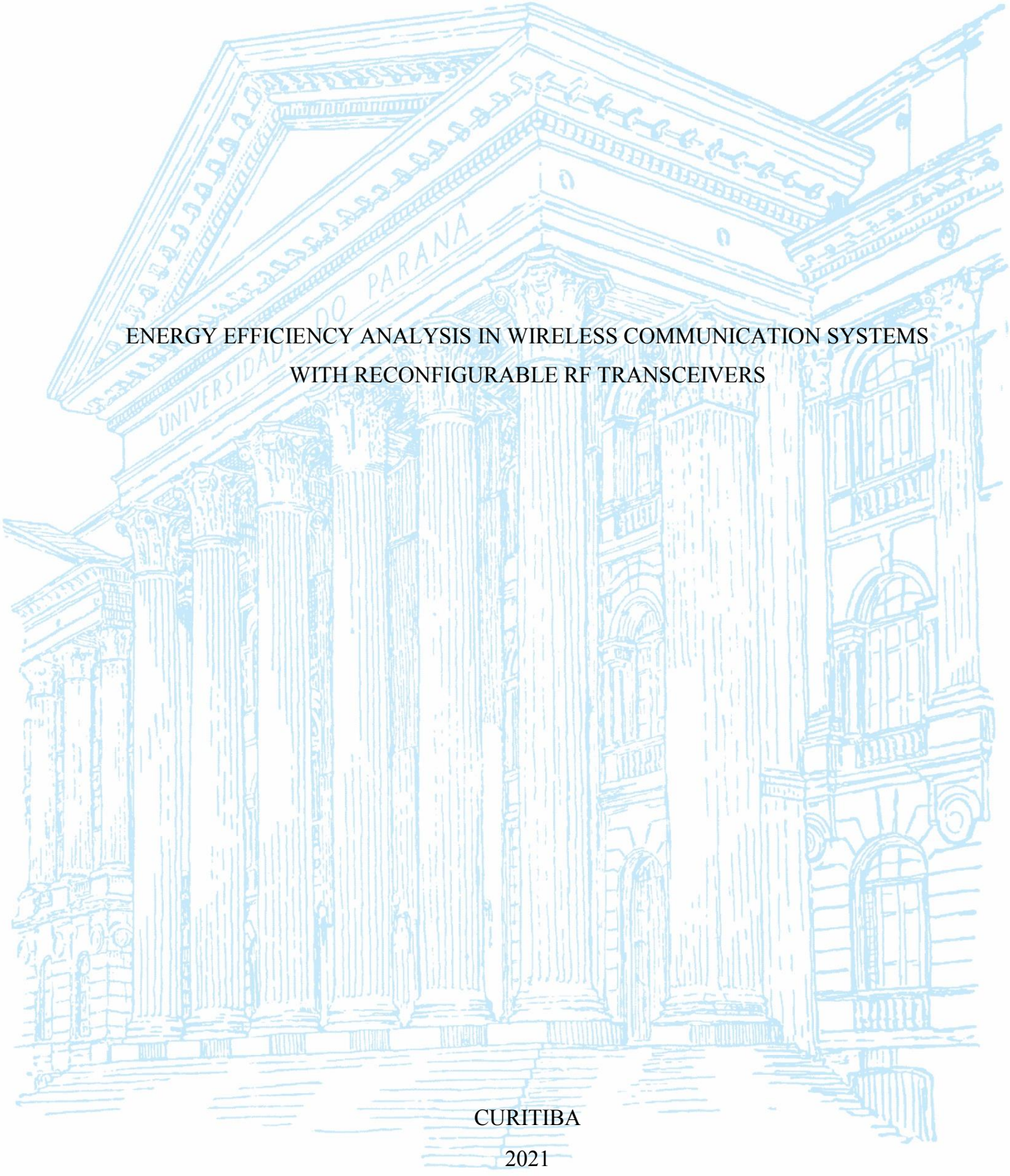

ENERGY EFFICIENCY ANALYSIS IN WIRELESS COMMUNICATION SYSTEMS WITH RECONFIGURABLE RF TRANSCEIVERS

CURITIBA

2021

EDSON LEONARDO DOS SANTOS

ENERGY EFFICIENCY ANALYSIS IN WIRELESS COMMUNICATION SYSTEMS WITH RECONFIGURABLE RF TRANSCEIVERS

Tese apresentada ao curso de Pós-Graduação em Engenharia Elétrica, Área de Concentração: Sistemas Eletrônicos, Setor de Tecnologia, Universidade Federal do Paraná, como requisito parcial à obtenção do título de Doutor em Engenharia Elétrica.

Orientador: Prof. Dr. André Augusto Mariano

Coorientador: Prof. Dr. Glauber Gomes de Oliveira Brante

CURITIBA

2021

Catalogação na Fonte: Sistema de Bibliotecas, UFPR
Biblioteca de Ciência e Tecnologia

S237e Santos, Edson Leonardo dos
Energy efficiency analysis in wireless communication systems with reconfigurable RF transceivers [recurso eletrônico] / Edson Leonardo dos Santos. – Curitiba, 2021.

Tese - Universidade Federal do Paraná, Setor de Tecnologia, Programa de Pós-Graduação em Engenharia Elétrica, 2021.

Orientador: André Augusto Mariano.
Coorientador: Glauber Gomes de Oliveira Brante.

1. Rádio frequência. 2. Sistemas de comunicação sem fio. I. Universidade Federal do Paraná. II. Mariano, André Augusto. III. Brante, Glauber Gomes de Oliveira. IV. Título.

CDD: 384.5

Bibliotecária: Vanusa Maciel CRB- 9/1928

MINISTÉRIO DA EDUCAÇÃO
SETOR DE TECNOLOGIA
UNIVERSIDADE FEDERAL DO PARANÁ
PRÓ-REITORIA DE PESQUISA E PÓS-GRADUAÇÃO
PROGRAMA DE PÓS-GRADUAÇÃO ENGENHARIA ELÉTRICA - 40001016043P4

TERMO DE APROVAÇÃO

Os membros da Banca Examinadora designada pelo Colegiado do Programa de Pós-Graduação em ENGENHARIA ELÉTRICA da Universidade Federal do Paraná foram convocados para realizar a arguição da tese de Doutorado de **EDSON LEONARDO DOS SANTOS** intitulada: **ENERGY EFFICIENCY ANALYSIS IN WIRELESS COMMUNICATION SYSTEMS WITH RECONFIGURABLE RF TRANSCEIVERS**, sob orientação do Prof. Dr. ANDRÉ AUGUSTO MARIANO, que após terem inquirido o aluno e realizada a avaliação do trabalho, são de parecer pela sua APROVAÇÃO no rito de defesa.

A outorga do título de doutor está sujeita à homologação pelo colegiado, ao atendimento de todas as indicações e correções solicitadas pela banca e ao pleno atendimento das demandas regimentais do Programa de Pós-Graduação.

CURITIBA, 28 de Maio de 2021.

Assinatura Eletrônica
28/05/2021 16:03:42.0
ANDRÉ AUGUSTO MARIANO
Presidente da Banca Examinadora

Assinatura Eletrônica
28/05/2021 15:54:18.0
EVELIO MARTÍN GARCÍA FERNÁNDEZ
Avaliador Interno (UNIVERSIDADE FEDERAL DO PARANÁ)

Assinatura Eletrônica
31/05/2021 08:56:12.0
PIETRO MARIS FERREIRA
Avaliador Externo (UNIVERSITÉ PARIS-SACLAY)

Assinatura Eletrônica
29/05/2021 09:42:43.0
JOAO LUIZ REBELATTO
Avaliador Externo (UNIVERSIDADE TECNOLÓGICA FEDERAL DO PARANÁ)

ACKNOWLEDGMENTS

First of all, I thank my family for all their support on this academic journey.

I am very grateful to my wife Luana for everything, my life partner.

I would like to express my deepest appreciation to my supervisors André Mariano, Glauber Brante and Bernardo Leite for believing in my potential and especially for leading me on this postgraduate path. Thank you for all your help, for sharing your knowledge and for your availability whenever I needed it.

My heartfelt acknowledgment to my friend Carlos Gouvea from the days of bachelor's, master's and doctorate degrees, for having embarked and sailed with me in these seas.

For the contributions, I thank my fellow researchers and professors at GICS.

My thanks to SENAI, UFPR and UTFPR, reference institutions in our country.

Finally, I would like to thank CAPES and CNPq for their financial support.

RESUMO

Alta eficiência energética (EE) é crucial para aplicações da Internet das Coisas que operam remotamente, uma vez que os nós sem fio são tipicamente alimentados por bateria. Diferentes técnicas de diversidade espacial tais com o uso de múltiplas antenas (MIMO) nos nós do transmissor e receptor, bem como o uso de comunicação cooperativa podem ser exploradas para melhorar a EE. Além disso, o uso de transceptores de rádio frequência (RF) reconfiguráveis são considerados uma solução interessante para sistemas com restrição de energia, pois permitem alterar o seu ponto de funcionamento, bem como o seu consumo de potência, adaptando-se aos diferentes requisitos de comunicação. Nessa tese, uma nova abordagem para economizar energia inclui no modelo do sistema de comunicação o uso de transceptores de RF reconfiguráveis. Mais especificamente, os componentes envolvidos em nossa estrutura de otimização de consumo de potência são o amplificador de potência (PA) no transmissor e o amplificador de baixo ruído (LNA) no receptor. Nosso objetivo é mostrar que os circuitos de RF baseados em operações multímodo podem melhorar significativamente a EE. Assim, realizamos uma seleção conjunta dos melhores modos de operação para os circuitos do PA e do LNA para diferentes esquemas de transmissão em dois cenários de rede: *i)* comunicação não-cooperativa em que os nós são equipados com múltiplas antenas, para a qual consideramos a seleção de antenas (AS) e a decomposição por valores singulares (SVD); e *ii)* comunicação cooperativa em que os nós são equipados com uma única antena, para a qual consideramos decodificação incremental e encaminha (IDF) por relé. Em nosso primeiro cenário proposto, comparamos os circuitos reconfiguráveis do PA e do LNA com amplificadores de RF não-reconfiguráveis do estado-da-arte disponíveis na literatura. Nesta comparação, ao explorar as características dos amplificadores reconfiguráveis de RF, mostramos uma melhora de EE de mais de 40% em distâncias curtas para as comunicações MIMO. Ao comparar os esquemas MIMO, a técnica AS apresenta melhor desempenho para distâncias mais curtas, enquanto que o SVD permite transmissões mais longas, pois explora todas as antenas disponíveis. Além disso, a otimização da eficiência espectral contribui para aumentar ainda mais a EE. Por fim, investigamos o efeito do número de antenas, em que a EE do AS sempre aumenta com o número de antenas, enquanto que o SVD apresenta um número ótimo de antenas. Para o segundo cenário, propomos uma análise de EE para o esquema IDF, auxiliada por um canal de retorno para realizar a seleção de relés. Além disso, comparamos o desempenho do IDF com os esquemas MIMO não-cooperativos. Os resultados mostram que uma melhor EE é obtida por meio de técnicas de seleção de antenas, principalmente quando aplicadas tanto no transmissor quanto no receptor. Também analisamos o impacto do relé na cooperação, uma vez que o nó do relé opera apenas se necessário, a maior parte da carga de reconfigurabilidade é do relé, enquanto os modos de operação do PA e do LNA tendem a ser razoavelmente fixados nos nós de origem e destino. Por fim, os resultados mostram que o número de relés contribui para alcançar transmissões de longa distância.

Palavras-chave: Eficiência Energética, Transceptores de RF Reconfiguráveis, Diversidade Espacial, Múltiplas Antenas, Comunicações Cooperativas.

ABSTRACT

High energy efficiency (EE) is crucial for Internet of Things applications that operate remotely, since wireless nodes are typically battery-powered. Different spatial diversity techniques such as the use of multiple antennas (MIMO) at the transmitter and receiver nodes, as well as the use of cooperative communication can be exploited to improve the EE. In addition, the use of radio frequency (RF) transceivers are considered an interesting solution for power-restricted systems, as they allow changing their operating point, as well as their power consumption, adapting to different communication requirements. In this thesis, a novel energy-saving approach includes in the communication system model the use of reconfigurable RF transceivers. More specifically, the components involved in our power consumption optimization framework are the power amplifier (PA) at the transmitter and the low noise amplifier (LNA) at the receiver. Our goal is to show that RF circuits based on multimode operation can significantly improve the EE. Thus, we perform a joint selection of the best operating modes for the PA and LNA circuits for different transmission schemes in two network scenarios: *i)* non-cooperative communication where the nodes are equipped with multiple antennas, for which we consider antenna selection (AS) and singular value decomposition (SVD) beamforming; and *ii)* cooperative communication where the nodes are equipped with single antenna, for which we consider incremental decode and forward (IDF) relaying. In our first proposed scenario, we compare the reconfigurable PA and LNA circuits with state-of-the-art non-reconfigurable RF amplifiers available in the literature. In this comparison, by exploiting the characteristics of reconfigurable RF amplifiers, we show an EE improvement of more than 40% at short distances for MIMO communications. When comparing MIMO schemes, the AS technique performs better for shorter distances, while the SVD allows for longer transmissions, as it exploits all available antennas. In addition, the optimization of the spectral efficiency contributes to further increase the EE. Finally, we investigate the effect of the number of antennas, in which the EE of AS always increases with the number of antennas, while SVD presents an optimal number of antennas. For the second scenario, we propose an EE analysis for the IDF scheme, aided by a feedback channel to perform relay selection. In addition, we compare the performance of the IDF with non-cooperative MIMO schemes. The results show that a better EE is obtained through antenna selection techniques, especially when applied at both transmitter and receiver. We also analyze the impact of the relay on cooperation, as the relay node operates only if necessary, most of the reconfigurability charge ends up at the relay, whereas the PA and LNA operating modes tend to be reasonably fixed at the source and destination nodes. Finally, results show that the number of relays contributes to achieving long distance transmissions.

Keywords: Energy Efficiency, Reconfigurable RF Transceivers, Spatial Diversity, Multiple Antennas, Cooperative Communications.

LIST OF FIGURES

LIST OF TABLES

LIST OF ABBREVIATIONS

3GPP	third-generation partnership project
4G	fourth-generation
5G	fifth-generation
ACK	acknowledgement
ADC	analog-to-digital converter
AS	antenna selection
AWGN	additive white Gaussian noise
BER	bit error rate
CMOS	complementary metal-oxide-semiconductor
CSI	channel state information
CSMA-CA	carrier sense multiple access with collision avoidance
DAC	digital-to-analog converter
DNC	dynamic network coding
EE	energy efficiency
FDSOI	fully-depleted silicon-on-insulator
GDNC	generalized dynamic network coding
GND	ground reference
IDF	incremental decode and forward
IF	intermediate frequency
IoT	Internet of Things
LNA	low noise amplifier
LO	local oscillator
LTE-M	long term evolution for machines
LUT	look-up table
M2M	machine-to-machine
MIMO	multiple antennas
mMTC	massive machine-type communication
NACK	negative acknowledgement
NB-IoT	narrowband-IoT
NLOS	non-line-of-sight
PA	power amplifier
PAPR	peak-to-average power ratio
QAM	quadrature amplitude modulation
QoS	quality of service
RF	radio frequency
SE	spectral efficiency
SISO	single antenna
SNR	signal-to-noise ratio
SVD	singular value decomposition
SWIPT	wireless information and power transfer
VDD	supply voltage

LIST OF SYMBOLS

S	source node
D	destination node
R_K	relay node
K	number of relays
N_i	available number of antennas at the transmitter
N_j	available number of antennas at the receiver
n_i	active number of antennas at the transmitter
n_j	active number of antennas at the receiver
$P_{\mathrm{PA},i,\mathrm{mode}}$	power consumption of the reconfigurable PA
$P_{\mathrm{LNA},j,\mathrm{mode}}$	power consumption of the reconfigurable LNA
$P_{\mathrm{TX},i}$	power consumption of the other non-reconfigurable circuits at the transmitter
$P_{\mathrm{RX},j}$	power consumption of the other non-reconfigurable circuits at the receiver
$G_{\mathrm{PA,mode}}$	PA power gain
$P_{i,\mathrm{mode}}$	PA transmission power
F	noise factor
NF	noise figure
$F_{j,\mathrm{mode}}$	receiver noise factor
$F_{\mathrm{LNA,mode}}$	LNA noise factor
$F_{\mathrm{SubsequentBlocks}}$	combined noise factor of the subsequent blocks at the receiver
$G_{\mathrm{LNA,mode}}$	LNA voltage gain
$\mathbf{y}_{ij}$	received signal vector
κ_{ij}	link budget relationship
$\mathbf{H}_{ij}$	matrix of quasi-static channel coefficients
$\mathbf{h}_{ij}$	channel fading vector
$\mathbf{x}_{ij}$	unit energy transmitted symbol vector
$\mathbf{w}_{ij}$	additive white Gaussian noise vector
N_0	unilateral thermal noise power spectral density
A	total antenna gains
λ	wavelength
f_{c}	carrier frequency
L	link margin
d_{ij}	distance between communicating nodes
α	path loss exponent
γ_{ij}	instantaneous SNR
$\|.\|_F$	Frobenius norm
$\bar{\gamma}_{ij}$	average SNR
P_j	received power
N	noise power
B	system bandwidth
I_{ij}	mutual information in the i-j link
R_{b}	information rate
ξ	spectral efficiency

$\mathcal{O}_{(\mathrm{sch})}$	outage probability
$\mathcal{T}$	system throughput
$\eta_{(\mathrm{sch})}$	energy efficiency
$\mathbf{I}_n$	identity matrix
λ_l	eigenvalues of $\mathbf{H}_{ij}\,\mathbf{H}_{ij}^{\dagger}$
M	constellation size of the M-ary QAM scheme
$\mathcal{O}^{\star}$	target outage probability
U	number of users
$\mathcal{E}_{\mathrm{f}}$	energy consumption for each successfully transferred bit
$\mathcal{E}_{\mathrm{fb}}$	energy consumption of the feedback frame
$\mathcal{E}_{\mathrm{broad}}$	energy consumption of the broadcast phase
$\mathcal{E}_{\mathrm{coop}}$	energy consumption of the cooperative phase
T_{b}	average transmission time per payload bit
T_{fb}	feedback time per payload bit for IDF and AS
T_{fbSVD}	feedback time per payload bit for SVD
R_{s}	symbol rate
P	forward payload frame length
H	forward header frame length
O	forward overhead frame length
F	feedback frame length for IDF and AS
F_{SVD}	feedback frame length for SVD

CONTENTS

CHAPTER 1

INTRODUCTION

1.1 Motivation

Due to the huge market potential, the Internet of Things (IoT) remains one of the hottest topics of discussion today (BEHRTCH, 2021). According to (IoT-ANALYTICS, 2020), for the first time, in 2020 there were more IoT connections (11.7 billion) than non-IoT connections (9.9 billion). Besides that, more than 30 billion devices connected to the Internet are expected by 2025. So to sum up, IoT will continue to be the driving force in the field of telecommunications, enabling the transformation of industry and society.

Many fifth-generation (5G) services are based on broadband communications and, progressively, the main IoT use cases are being addressed. However, it is noted that due to the diversity of the IoT application requirements, in addition to 5G, long term evolution for machines (LTE-M) and narrowband-IoT (NB-IoT), two inherited third-generation partnership project (3GPP) technologies based on fourth-generation (4G) LTE, will continue to play a role in addressing the wide range of requirements (OSSEIRAN et al., 2020). The NB-IoT belongs to the category of low-power wide-area networks (LPWAN) and has been standardized in order to support massive machine-type communication (mMTC), for which the market is in full growth. According to (CISCO, 2020), the share of machine-to-machine (M2M) connections will grow from 33% in 2018 to 50% by 2023 and there will be 14.7 billion M2M connections by 2023. This fast growth implies the challenge of satisfying the quality of service (QoS) requirements for mMTC in 5G and beyond (LU; ZHENG, 2020). Moreover, the main specifications of IoT use cases become low-cost, low-size, low-complexity and low-power devices (i-SCOOP, 2019).

Massive IoT networks must require connected devices that use embedded electronics such as microprocessors, sensors and actuators in order to collect, share and act on data they acquire

from their local environments. Moreover, in wireless communications, each device is equipped with a set of radio frequency (RF) transceivers and antennas, typically powered by batteries or even by solar cells that can seldom or never be recharged, so one of the most noteworthy concerns of these massive networks is the efficient use of limited power sources. Therefore, in such systems where energy is at a premium, minimizing power consumption improves the energy efficiency (EE). With that in mind, the seek for energy-efficient solutions becomes the main motivation of this research work.

1.2 Background

As a medium for communication, the wireless channel imposes difficulties in propagating the signal, which implies in a random variation of the received signal. Due to the fading of the wireless channel, it is common to use devices that consume large amounts of power for reliable communication. One of the most promising techniques to mitigate the effects of fading is the so-called spatial diversity (GOLDSMITH, 2005), in which the information messages can be transmitted via independently fading paths, decreasing the probability of simultaneous fading. As illustrated in Fig. 1.1(a), the diversity order can be exploited through multiple antennas (MIMO) at the source and destination nodes, which improves the link reliability, so that less transmission power can be required during communication (GOLDSMITH, 2005). It is worth noting that great advances in the design of antenna arrangements have been reached in recent years (MAXIM INTEGRATED, 2011; TEXAS INSTRUMENTS, 2017), making the use of MIMO on small nodes possible. On the other hand, multiple antennas also implies in multiple RF chains, consuming more power at the circuit level. Alternatively, as illustrated in Fig. 1.1(b), cooperative communications based on the relay channel (MEULEN, 1971; COVER; GAMAL, 1979) can also achieve diversity order, in which spatially distributed nodes cooperate to improve link quality, thereby requiring less transmission power from wireless nodes (SENDONARIS; ERKIP; AAZHANG, 2003; LANEMAN; TSE; WORNELL, 2004). However, more nodes entails the same drawback as MIMO, that is, more power consumption due to the number of nodes involved in the communication process.

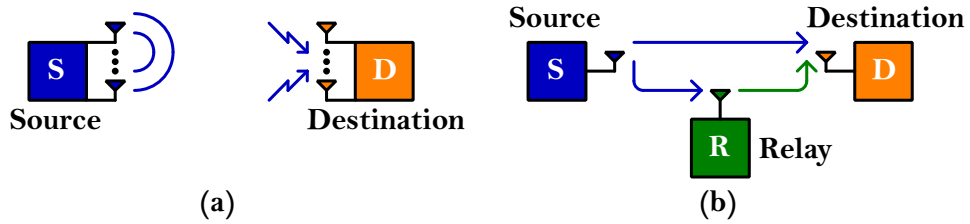

Figure 1.1: (a) MIMO communication and (b) cooperative communication.

In particular, when the nodes are far apart, the consumption is dominated by the transmission power. However, when the nodes are closer to each other, the circuitry consumption becomes relevant (CUI; GOLDSMITH; BAHAI, 2004). Therefore, both the transmission power and the power consumed by the circuits must be taken into account. What is mostly observed, is that RF transceivers are usually designed with a fixed operating point, considering the worst-case scenario in compliance with a communication standard. However, the high performance of the hardware is not always required during system operation, so that electronic circuits are often over-specified. Thereby, in situations where the communication link is better than the worst-case assumption, circuits end up consuming more power than necessary, compromising the system's energy efficiency. For this reason, if RF transceivers can change the operating point of their circuits, i.e., reduce the performance without impairing the quality target for the communication system, then energy savings can be achieved (SANTOS; LEITE; MARIANO, 2015; SOUZA; MARIANO; TARIS, 2017).

1.3 Research Goal

This work proposes the EE analysis in wireless communication systems with spatial diversity and reconfigurable RF transceivers. We combine the design of energy-efficient multimode PA and LNA circuits with the spatial diversity gains through MIMO and cooperative communications. Thus, our goal is to show that this approach may be a key solution towards improving the EE.

1.3.1 Delimitation

In this work, we address only one reconfigurable circuit at the transmitter and one at the receiver, since an RF transceiver has several building blocks and integrating all of them into the system model would increase the complexity. Based on our prior knowledge of reconfigurable circuits, we consider the power amplifier (PA) at the transmitter and the low noise amplifier (LNA) at the receiver, exploiting different operating modes that impact the power consumption. Therefore, this thesis is limited to the circuits responsible for amplifying the RF signal. Moreover, we consider a single operating point with fixed power consumption for the other circuits in the RF transceiver chain.

1.3.2 Objectives

The specific objectives of this thesis are listed as follows:

- Conduct a theoretical study on spatial diversity techniques;
- Conduct a survey of transmission schemes based on MIMO and cooperative communications;
- Conduct a theoretical study on RF transceivers;
- Conduct a survey of reconfigurable PA and LNA circuits;
- Model the communication system to integrate reconfigurable circuits;
- Develop an algorithm in order to maximize the EE;
- Perform an analysis of EE in different transmission schemes with reconfigurable circuits.

1.4 Methodology

In this work, we combine the reconfigurable capability of RF transceivers with spatial diversity transmission schemes. Thus, we analyze the EE in two network scenarios: *i)* non-

cooperative communication where the nodes are equipped with multiple antennas and *ii)* cooperative communication with multiple relays where the nodes are equipped with single antenna. In the first scenario, we consider antenna selection (AS), singular value decomposition (SVD) beamforming and single antenna (SISO) for comparison purposes. In the second scenario, we consider incremental decode and forward (IDF) relaying and non-cooperative schemes with multiple antennas nodes for comparison purposes.

In order to maximize the EE of the communication system, we carry out a joint selection of the best operating modes of the PA and LNA circuits, given a QoS constraint at the receiver, expressed in terms of a maximal allowed outage probability[1]. Notice that, in addition to employing the reconfigurable RF amplifiers into the communication system model, we also seek to maximize the EE for the MIMO scenario by optimizing the spectral efficiency (SE) for MIMO schemes. Moreover, it is worth mentioning that for the second proposed scenario, we also provide an EE analysis when the energy consumed by the feedback channel is considered.

The procedure adopted in this work to analyze EE in the two proposed network scenarios follows a sequence of steps. First, we model the communication system to integrate the reconfigurable RF amplifiers. Next, we formulate the closed-form expressions for outage probability and EE for each transmission scheme. Then, we define an algorithm for each communication scenario that combines the transmission schemes with the PA and LNA operating modes, in addition to other parameters such as the number of antennas, the number of relays and the SE. Finally, according to our proposed optimization problem, we present and discuss the EE results for the different schemes under test.

1.5 Thesis Layout

The thesis is organized as follows. In Chapter 2, we present the state-of-the-art on the use of spatial diversity techniques, focusing mainly on MIMO and cooperative communications.

[1] In wireless systems, there is typically a target minimum received power level, in which performance becomes unacceptable. Outage probability is defined as the point at which the receiver power value falls below the required threshold information rate (GOLDSMITH, 2005).

Through this literature review, we found the use of several techniques that seek to improve the EE of wireless communication systems. Next, we overview the literature on RF transceivers focusing on reconfigurable PA and LNA designs, in which we present their main performance features. In Chapter 3, we detail the reconfigurable RF amplifiers chosen to be used in this work. In addition, we model the communication system to include the operating parameters of the PA and LNA circuits.

In Chapter 4 we employ non-cooperative MIMO schemes, while in Chapter 5 we extend the analysis to cooperation. In Chapter 4, we initially present the closed-form expressions for outage probability and EE for SISO, AS and SVD schemes. Then, we introduce our optimization problem and detail the algorithm that will be used in the simulations. After that, we present the EE results for three test scenarios: *i)* with fixed SE, *ii)* with optimized SE and *iii)* some considerations with respect to the optimization of the number of antennas. In Chapter 5, we compare a cooperative SISO approach, employing the IDF scheme and multiple relays, with non-cooperative MIMO schemes. Then, we model the EE by considering a transmission with a feedback channel, which is required to perform relay selection. Next, we present the benchmark MIMO schemes. In addition, we develop our optimization problem and the algorithm to employ the IDF scheme. After that, we present some numerical examples to demonstrate the performance of the IDF in relation to the non-cooperative MIMO schemes, in addition to some considerations about the number of relays.

Finally, Chapter 6 exposes our perspectives for future works, lists published papers and concludes this thesis.

CHAPTER 2

LITERATURE REVIEW

2.1 Spatial Diversity

To attenuate the impairments imposed by the wireless channel, different techniques are usually employed to make the communication system more reliable, thus enabling the EE improvement. In the following, we present several works based on spatial diversity.

Our initial research targets MIMO techniques to maximize the EE, of which AS and SVD beamforming are addressed in Chapter 4. On the one hand, MIMO communication can considerably improve the signal-to-noise ratio (SNR) when compared to SISO (GOLDSMITH, 2005). Hence, the use of MIMO techniques may require less transmission power than SISO for the same performance requirement. On the other hand, it is important to note that one antenna in MIMO systems usually corresponds to one RF chain and, therefore, a large number of RF chains not only consume a large amount of power, but also increase the cost.

AS is deemed a key technique (MOLISCH; WIN, 2004), since AS yields the same diversity gains of MIMO, but with lower power consumption at the circuit level, due to the reduced number of RF chains. Therefore, different approaches have been proposed using the AS technique. To exemplify, four AS schemes were proposed by (MARINELLO et al., 2020) to improve the EE in extra large MIMO communication. While in (KHALILI et al., 2020), the EE was analyzed in two AS scenarios and the authors work with resource allocation for the EE maximization. By switching the RF chain among multiple antennas, the authors in (JIN et al., 2019) showed that the trade-off between EE and SE can be achieved with the AS scheme. Moreover, according to (LIU; DU; SUN, 2017), the EE-SE trade-off can be achieved with respect to the transmission power and the number of transmission antennas. In (OUYANG et al., 2020), the EE was analyzed applying the AS scheme at the receiver, in which an optimum number of

active antennas was found to maximize the EE. While in (ESKANDARI et al., 2018; GUSTAVSSON et al., 2021), the authors proposed a joint AS with power allocation optimization for energy-efficient MIMO systems. Moreover, there are some algorithms focused on increasing the AS performance, such as reversing petri nets (SILJAK; PSARA; PHILIPPOU, 2019), based on machine learning (YANG et al., 2019), hybrid precoding (GE; ZHANG, 2019), monte carlo tree search (CHEN et al., 2019) and greedy algorithms (MENDONÇA et al., 2020).

Alternatively, beamforming techniques can be used in antenna arrays to transmit or receive directional signals, in which the link reliability can be increased to improve the EE. For example, the joint transmit beamforming and AS technique was proposed by (ZHAO et al., 2018). In (HANNULA et al., 2018), the feasibility of implementing a tunable antenna system with integrated RF transceivers was discussed. While in (CICCIA; GIORDANENGO; VECCHI, 2019), energy savings are shown by integrating reconfigurable antennas into ultra low-power RF platforms. In (DU; SHOKRI-GHADIKOLAEI; FISCHIONE, 2020), the authors considered power allocation and transmit beamforming scheme. Whereas the (YU et al., 2019) showed three power allocation schemes with beamforming and AS for the EE maximization. In (KRAUSS et al., 2019), the authors analyzed the EE and SE applying the AS and beamforming schemes. Moreover, simultaneous wireless information and power transfer (SWIPT) technique has also been addressed in MIMO system deployments, in order to prolong the lifetime of wireless nodes (CLERCKX et al., 2019; WANG; ASHIKHMIN; WANG, 2020).

The literature review continues with cooperative techniques to maximize the EE, with IDF relaying being addressed in Chapter 5. Cooperative communication is another alternative to achieve diversity gains, through sharing resources from different devices that use the same wireless channel (MEULEN, 1971; COVER; GAMAL, 1979; SENDONARIS; ERKIP; AAZHANG, 2003; LANEMAN; TSE; WORNELL, 2004). The performance of cooperative and non-cooperative schemes was discussed by (BRANTE; KAKITANI; SOUZA, 2011; TUAN; KIM; LEE, 2018), whose results showed that by exploiting the feedback channel in cooperative schemes such as IDF relaying, it can be more energy-efficient than cooperative schemes without feedback and non-cooperative schemes. Similar to MIMO, cooperative com-

munication also has a disadvantage in relation to the power consumption of circuits, that is, it increases according to the number of nodes. In this context, relay selection can save energy, since a relay with the best channel condition is selected to assist in the communication process (BLETSAS et al., 2006). Note that the selected relay transmits to the destination using one channel, thus minimizing the number of channels without sacrificing the diversity gain. Different relay selection techniques available in the literature have been discussed in (LIANG et al., 2013). In addition, a study of different algorithms for relay selection was carried out by (GHASRI et al., 2020).

The system performance analysis with joint multiple relays and antennas was also investigated. In (PERON; BRANTE; SOUZA, 2015), the authors proposed an energy-efficient distributed power allocation with multiple relays and AS. While in (KAZEMI; MOHAMMADI; DUMAN, 2020), the relay selection was employed considering a cooperative MIMO system. SWIPT relays were adopted in (GUO; ZHOU; ZHOU, 2020) to improve the EE. In (SALIM et al., 2019), it was proposed optimum resource and power allocation with relay selection for energy harvesting scenarios. While in (ZOU; ZHU; JIANG, 2020), the authors also considered an energy harvesting relay system, in which a joint power splitting and relay selection is employed to improve the system performance.

2.2 RF Transceivers

As aforementioned, through spatial diversity it is possible to make the wireless channel more robust and, therefore, less transmission power may be required, thus improving the EE. However, one factor that cannot be neglected is the total power consumption required by the transmitter and receiver nodes. In many scenarios, wireless nodes operate on low-charge batteries, which can be difficult and expensive to recharge or replace. Therefore, the lifetime of a node depends mainly on the amount of energy available in its battery. Although semiconductor technologies have enabled significant improvements in the construction of devices with higher processing capacity and storage space, the development of new battery improvements is growing slowly or stagnating (U.S. DEPARTMENT OF ENERGY, 2020). Consequently, this not

only increases the demand for new energy-efficient solutions, but also increases the challenge of circuit designers in terms of optimizing the power consumption of RF transceivers.

In order to transmit and receive RF signals, wireless communication systems require devices with specific circuits. Fig. 2.1 shows a simplified block diagram for the transmitter and the receiver (STEER, 2010), including amplifiers, filters, mixers, digital-to-analog converter (DAC), analog-to-digital converter (ADC) and frequency synthesizer. Basically, RF transceivers can be divided into three parts; radio frequency stage (for the RF signal amplification process), intermediate frequency stage (for the frequency up/down conversion process) and baseband stage (for the modulation and demodulation process). Following the receive path, the signal coming from the antenna is filtered and amplified before entering the mixer, which down-converts the RF signal to an intermediate frequency (IF), followed by an IF filter and IF amplifier. Then, the ADC converts the analog signal into a digital signal, so that the demodulation can be performed. On the other hand, in the transmit path, the digital signal is converted to analog signal by the DAC, followed by an IF filter before entering the mixer, which up-converts the modulated signal to the desired carrier frequency. Then, the RF signal is filtered and amplified towards the antenna at the required transmission power level. Futhermore, a frequency synthesizer to generate the local oscillator (LO) frequency completes the RF transceiver.

The PA and LNA are responsible for amplifying RF signals and, therefore, the most critical active circuits of the transmitter and receiver, respectively. These amplifiers are typically designed for the worst operating scenario, however, when high performance is not required during communication, the device's power consumption becomes excessive. In this context, a significant improvement in battery lifetime can be achieved if the device is able to reconfigure itself according to the operating scenario. Normally, each building block of an RF transceiver follows a different architecture, which aims to meet the minimum specifications of a targeted application. In this work, our research focuses on reconfigurable PA and LNA circuits with different power consumption modes, to operate at the 2.4 GHz band. Next, we present the main design metrics for the PA and LNA, in addition to the foremost works found in the literature.

At the transmitter, the PA ends up consuming a large amount of power to amplify the

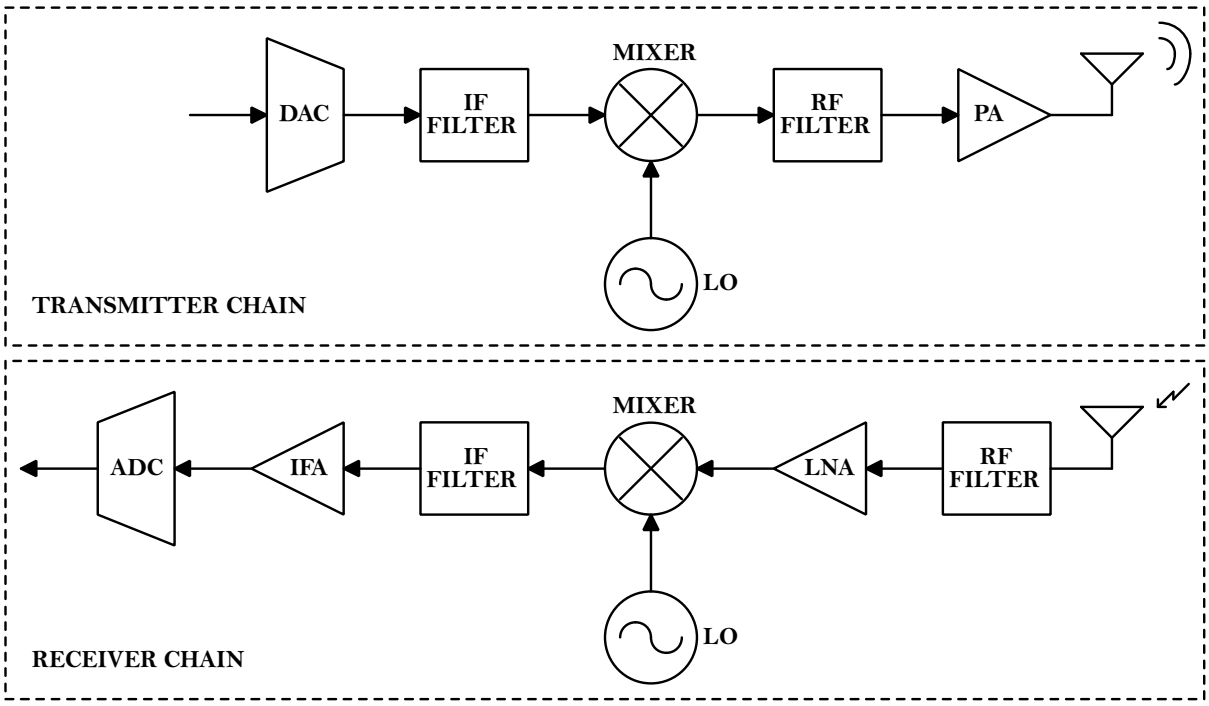

Figure 2.1: Simplified block diagram of an RF transceiver. Adapted from (STEER, 2010).

signal that will be transmitted by the antenna (RUIZ; PÉREZ, 2014). Thus, adjusting the PA parameters is crucial to achieve high energy efficiency; even more so under modulated signals, which typically have a high peak-to-average power ratio (PAPR) that limits the average output power of the transmitter device. Notice that in the design of a PA, metrics such as power gain, output power, stability, linearity and efficiency are generally the most important (CRIPPS, 2006). However, it is not possible to optimize all these parameters at the same time and the most designs focus on a trade-off between some of them. To create different operating modes, both the power gain and the output power or either can be reconfigured to adjust the performance as well as the power consumption of the PA.

For instance, a fixed gain stage with a reconfigurable power stage was proposed by (SANTOS; MARIANO; LEITE, 2016), which achieves a power gain of 13.5 dB and an output power of 6 dBm in the lowest power mode, consuming 171 mW. For the highest power mode, a power gain of 21.1 dB and an output power of 18.9 dBm are obtained by consuming 415 mW. The PA in (SANTOS et al., 2017) also consists of two stages, the first with variable power gain and the second with fixed output power. In this PA, the gain ranges from 22.4 dB in the lowest gain mode to 31 dB in the highest gain mode, so that the power consumption varies from 171 to

196.2 mW, besides to reaching an output power of 13.3 dBm. The works of (SANTOS; MARIANO; LEITE, 2016) and (SANTOS et al., 2017) have been jointly extended in order to consider both stages being reconfigurable (TARUI et al., 2018). Such combination is controlled by six digital switches, three at each stage, yielding 64 possible operating modes with different levels of power gain, output power and power consumption. The PA in (TARUI et al., 2018) admits the power gain ranges from 10.1 to 31 dB, while the output power varies from 2.1 to 16.9 dBm, with a power consumption of 119 to 394 mW.

Besides that, a twelve-mode PA with reconfigurable output matching network and supply voltage selection was proposed by (MODESTO et al., 2019). This PA achieves a power gain of 18.3 dB and an output power of 10.1 dBm, consuming 94.7 mW in the lowest power mode. For the highest power mode, a power gain of 22.5 dB and an output power of 18.2 dBm are obtained with a power consumption of 341.4 mW. In (GILASGAR; BARLABÉ; PRADELL, 2019), the authors proposed a PA with reconfigurable load-impedance matching, in which it reaches 16.8 dBm in the output power and 7.9 dB in the power gain for a supply voltage of 3 V, and an output power of 18.7 dBm with a power gain of 9.7 dB for a supply voltage of 4 V. While in (GKOUTIS; KOLIOS; KALIVAS, 2019), the achieved output power of the PA ranges from -4.6 to 14.2 dBm with a maximum power gain of 25.1 dB. In (SANTOS; LEITE; MARIANO, 2020), the PA provides an output power of 16.8, 18.1 and 19.9 dBm with a power gain of 8.1, 9.6 and 8.8 dB, by consuming 125.1, 183 and 296.5 mW for each operating mode, respectively. In addition, another PA with three operating modes was presented by (BANERJEE; DING; HEZAR, 2020), in which the peak output power varies from 11.7 to 31.6 dBm and the power consumption ranges from 270.8 to 642.2 mW.

At the receiver, the sensitivity is dictated by the LNA in terms of noise figure and gain (FRIIS, 1944), due to its position at the beginning of the receiver chain. Therefore, the LNA should be designed with high gain to sufficiently reduce the noise contribution of the subsequent blocks (NXP, 2013). Consequently, the performance requirements of the other building blocks can be relaxed to save energy. Besides to the low noise requirements, high linearity is also important in order to amplify the received signal with minimal distortion. However, it is important

to emphasize that linearity was not taken into account in this work, since we did not consider in our analysis an environment with interferences and, therefore, we assume that the RF amplifiers operate in the linear zone. Although the LNA power consumption is much lower than the PA, the proper adjustment of the LNA parameters may help the PA to operate in lower consumption modes (SANTOS et al., 2019). Typically, reconfigurable LNA designs exploit current or voltage control, impedance variation and feedback control to adjust their parameters.

For instance, the LNA proposed by (SOUZA; MARIANO; TARIS, 2017) has three operating modes and the circuit design is based on a complementary current-reuse common source amplifier, combined with a low-current active feedback. In high linearity mode, the LNA achieves a minimum noise figure of 2 dB and a voltage gain of 21.1 dB with 7 mW of power consumption. In low-power mode, it draws 1.5 mW, providing a 2.6 dB noise figure and a 21 dB voltage gain, so that the overall LNA consumption can be reduced by more than 21%. Another three-mode LNA was proposed by (ZAINI et al., 2017; ZAINI-DESEVEDAVY et al., 2018), in which the circuit design consists of a common gate topology exploiting transistor body biasing while the LNA parameters are reconfigurable by changing the supply voltage. Thus, the voltage gain is 16.8 dB, 18.8 dB and 21.5 dB, whereas the noise figure is 7.3 dB, 6.7 dB and 6.3 dB, with a power consumption of 300 μW, 600 μW and 900 μW, respectively for each operating mode.

Besides that, current reuse and forward-body-bias techniques were employed to reduce the power dissipation in the LNA presented by (BISHT; QURESHI, 2019). This reconfigurable LNA allows for five operating modes and achieves a power gain of 3.96 to 10.17 dB with a noise figure ranging from 3.77 to 5.34 dB and a power consumption of 1.61 mW. In (CHANG; SHIN, 2020), the authors presented a six-mode receiver, in which the gain can be controlled from 2 to 62 dB, while the noise figure is found between $2.5-3.0$ dB, by dissipating 3.55 mW. Moreover, two interesting LNAs can be found in the works of (WANG; HUANG; JIN, 2019; KUMAR; DUTTA; SAHOO, 2020), however, these recent LNAs have their parameters reconfigurable in band, that is, they can operate at different frequency bands in addition to the 2.4 GHz.

2.3 Summary of the Chapter

As well as the main goal of this research work, the EE has been investigated extensively in MIMO and cooperative scenarios, aiming to seek a better quality of transmission, while consuming the lowest possible energy. Under the MIMO point of view, the AS technique can be an interesting solution to increase the EE. The results presented by the state-of-the-art show that the AS stands out mainly when the network nodes are closer to each other, even outperforming transmissions with SISO nodes. On the other hand, MIMO beamforming is optimal in terms of outage probability, reaching longer communication distances. However, MIMO beamforming has low EE in short-range transmissions, since multiple RF chains consume more power at the circuit level. Motivated by this trade-off in relation to the communication distance, the EE of both schemes with reconfigurable RF amplifiers will be analyzed in Chapter 4. This EE analysis can be useful for future implementations that encompass different communication scenarios of wireless sensor networks and IoT.

In relation to cooperative communication, some protocols have been developed to obtain diversity, in which we can highlight the IDF relaying scheme, especially when considering the feedback channel, since better EE results can be achieved when compared to schemes without feedback and direct transmission. So, the EE of this scheme will be exploited with reconfigurable RF amplifiers in Chapter 5. Moreover, we consider multiple relays in the cooperative scenario, so that the relay selection is essential to save energy.

Although the power consumption of the transmitter and receiver chain is taken into account in most works based on spatial diversity, optimizing the transmission power is the main goal to improve the EE. Besides that, this collection of works does not exploit the characteristics of reconfigurable electronic circuits that can be used in RF transceivers to save energy. However, in the constant search for energy-efficient solutions, different possibilities need to be tested. In this context, combining the spatial diversity gains with reconfigurable RF transceivers becomes the main goal of this thesis, which will be detailed in the subsequent chapters.

Among the reconfigurable PA and LNA circuits found in the literature to operate at the

2.4 GHz band, we have selected amplifiers with features that meet the performance requirements of IoT applications (XIA; CHEN; YANG, 2020). That is, according to 3GPP release 12 (3GPP TR 36.888, 2013), for a transmission power of 23 dBm and for a occupied channel bandwidth of 180 kHz, it is considered a 5 dB receiver noise figure. Later, in 3GPP release 14 (3GPP TR 21.914, 2018), a lower 14 dBm power class was introduced for the use of low-charge batteries as well as device cost reduction.

To assess the EE in the MIMO and cooperative scenario and bearing those IoT specifications in mind, we chose the PA proposed by (TARUI et al., 2018), whose reconfiguration capacity has 64 different operating modes reaching an interesting variation in the transmission power from 2.1 to 16.9 dBm and a power consumption that can be reduced by more than 30%. In addition, we chose the LNA in (ZAINI et al., 2017), even if the noise figure is between $1-2$ dB above the specification, this is the LNA that performs the lowest power dissipation, while presenting an interesting gain for each operating mode. In the next chapter, we will detail these reconfigurable PA and LNA circuits.

CHAPTER 3

RECONFIGURABLE DESIGNS AND SYSTEM MODEL

In this work, we consider two network scenarios: *i)* non-cooperative communication with MIMO nodes and *ii)* cooperative communication with SISO nodes; composed of one source node denoted by S, one destination node denoted by D and K relay nodes denoted by R_K, where $K \geq 0$[1]. Notice that the first network scenario is dealt with in Chapter 4, following the work presented in (SANTOS et al., 2019). While the second proposed scenario is addressed in Chapter 5, which is based on the work presented in (SANTOS et al., 2020). Let us consider the RF signal transceiver chain represented by the block diagram in Fig. 3.1, in which the PA and LNA are able to reconfigure their operating performance, while the other building blocks have fixed operating point and fixed power consumption. We use capital letters N_i and N_j to represent the available number of antennas at the transmitter and receiver, respectively; and lower case letters n_i and n_j to denote the active number of antennas at each node. It is important to remark that each RF chain is assembled with a single antenna. Moreover, $P_{\mathrm{PA},i,\mathrm{mode}}$ and $P_{\mathrm{LNA},j,\mathrm{mode}}$ are the power consumed by the reconfigurable PA and LNA circuits, which depend on their respective operating modes; whereas $P_{\mathrm{TX},i}$ and $P_{\mathrm{RX},j}$ represent the power consumption of the other non-reconfigurable circuits at the transmitter and receiver chain.

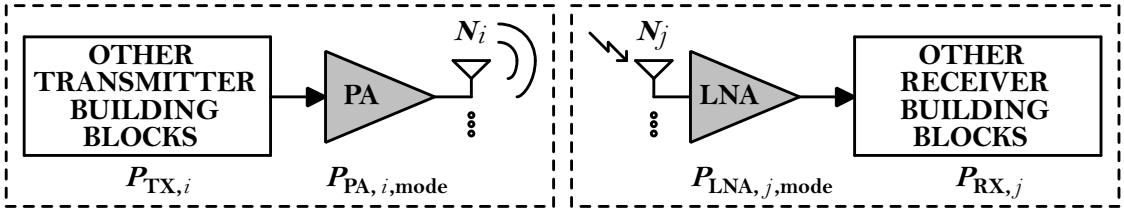

Figure 3.1: RF transceiver, in which the circuits in gray are multimode designs.

[1]It is important to note that Chapter 4 considers the particular case of $K = 0$ relays, since we seek only to compare non-cooperative schemes.

3.1 Reconfigurable Power Amplifier (PA)

Typically, the PA is the most power-hungry block of the transmitter and, therefore, we consider the reconfigurable parameters of this circuit to be inserted into the system model. The adopted PA follows (TARUI et al., 2018), which is a two-stage class AB based on the cascode topology, developed in an 130 nm CMOS technology.

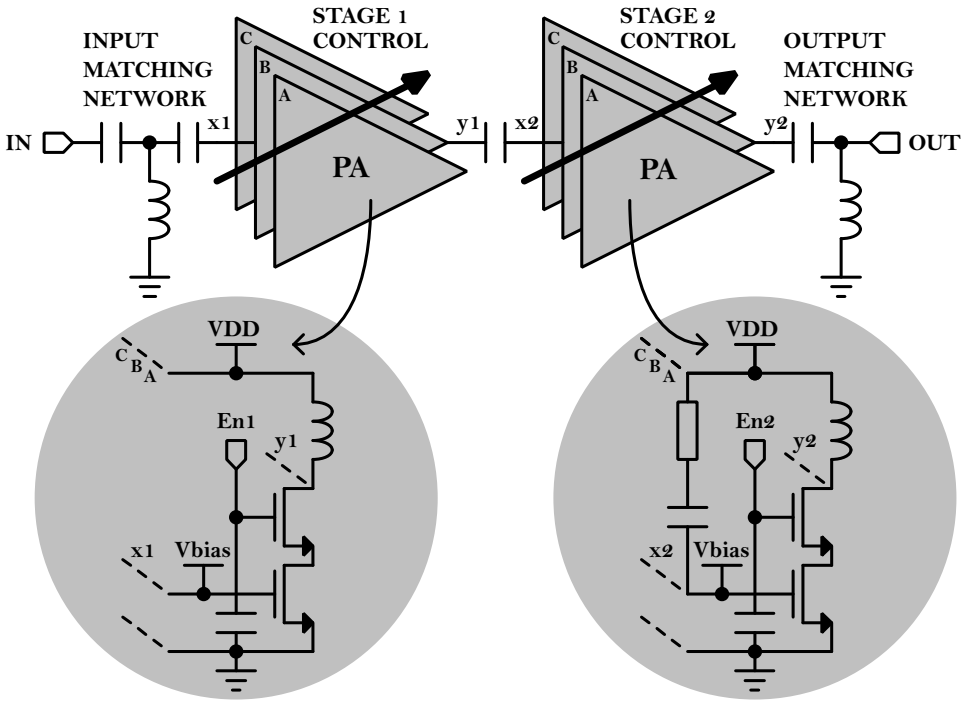

Figure 3.2: Multimode PA circuit design proposed in (TARUI et al., 2018) with gain and power control (bias circuit is omitted).

Fig. 3.2 illustrates the PA design featuring a power gain stage, an output power stage and two impedance matching networks. The first stage is responsible for the gain control, while the second is a power control stage. In addition, the circuit topology has three cascode cells (A, B and C) at each stage that are controlled by six digital switches (En1A, En1B, En1C, En2A, En2B and En2C). Each switch acts on a cascode cell that is enabled with VDD = 1.8 V and disabled with VDD = 0 V (GND). Therefore, for each activated structure, the width of the effective channel resulting from the transistors increases, and thus the gain and the power increases as well. The combination of these cascode structures provides distinct amplifying characteristics for each cell, yielding 64 possible operating modes. Nevertheless, only 9 out of

the 64 operating modes have been selected in this work, those that offer the best performance advantages in terms of power gain, output power and power consumption.

Table 3.1 summarizes the post-layout results for each of the selected operating modes. The operating mode 1 indicates the performance with the lowest power consumption, while operating mode 9 represents the high-performance mode. As we can observe, the power gain varies from 10.1 to 31 dB, the output power at the 1 dB compression point varies from 2.1 to 16.9 dBm, whereas the power consumption can be as low as 119 mW, up to 394 mW in the high-performance mode.

Table 3.1: Characteristics of the proposed PA for each operating mode at 2.4 GHz.

Operating Mode	Power Gain ($G_{\mathrm{PA,mode}}$) [dB]	Transmission Power ($P_{i,\mathrm{mode}}$) [dBm]	Power Consumption ($P_{\mathrm{PA},i,\mathrm{mode}}$) [mW]
1	10.1	2.1	119
2	15.0	4.1	126
3	18.0	7.5	153
4	23.2	8.1	166
5	26.1	12.3	223
6	26.8	13.3	245
7	30.1	15.3	310
8	30.9	15.9	337
9	31.0	16.9	394

Usually, conventional linear PAs achieve high efficiency close to the peak output power. However, in modulated communication signals, these PAs operate most of the time at power back-off and, consequently, the efficiency drops quickly at backed-off power levels. Thus, PAs based on multimode operation are more propitious to improve the efficiency at power back-off, since it can be switched to a lower power level to regain efficiency. The linearity characterization of simplified versions of this PA in the presence of modulated signals for the IEEE 802.11n, IEEE 802.11ax, IEEE 802.15.4 and LTE communication standards can be found in (RIOS et al., 2016) and (MODESTO et al., 2018).

It is worth noting that in the case of multiple active RF chains, we assume that the transmission power is uniformilly distributed, so that all PAs operate in the same mode.

3.2 Reconfigurable Low Noise Amplifier (LNA)

Following the antenna-filter block, the LNA dictates the receiver sensitivity and, therefore, we consider the reconfigurable parameters of this circuit to be inserted into the system model. The employed LNA in (ZAINI et al., 2017) was designed for ultra low-power applications and implemented in fully-depleted silicon-on-insulator (FDSOI) 28 nm technology.

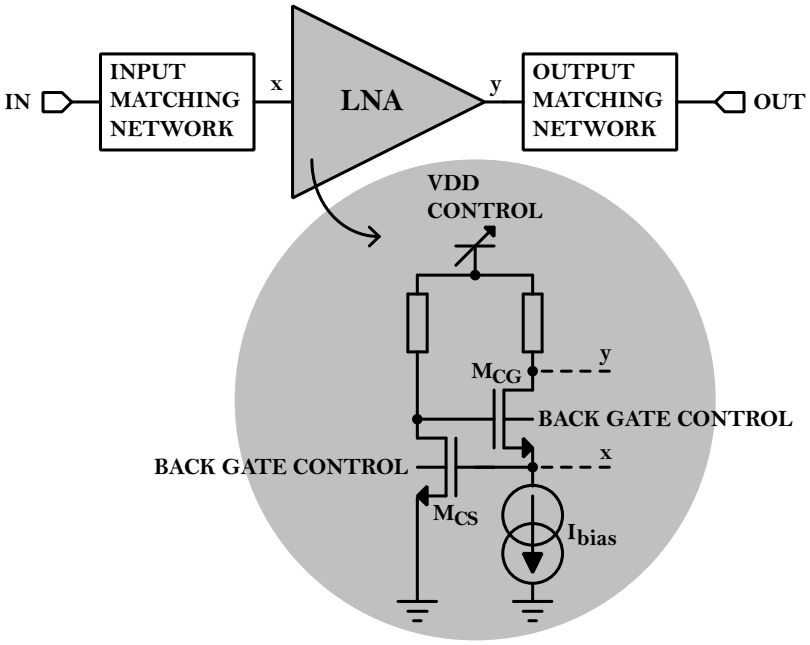

Figure 3.3: Multimode LNA circuit design proposed in (ZAINI et al., 2017) with back gate control (bias circuit is omitted).

A simplified schematic of the adopted LNA is reported in Fig. 3.3. Interestingly input matching is directly achieved by the common gate ($\mathrm{M_{CG}}$) stage, and controlled by the bias current ($\mathrm{I_{bias}}$). Unlike conventionnal LNA topologies, the proposed topology does not embed passive devices, such as inductors for input/output matching, dramastically reducing its silicon footprint. This feature reduces the implementation cost of a communication system. The amplifier parameters are reconfigurable via supply voltage. However, there is a threshold of VDD = 0.8 V where the parameters are acceptable and there is no other possibility of decreasing the supply voltage while maintaining the design requirements. Therefore, by tuning control through body biasing, the threshold voltage of the transistors is decreased and the power supply voltage can thus be reduced to 0.6 V with a back gate voltage of 2.0 V. This configuration en-

hances the available gain and enables a reasonable noise factor[2] under low-power constraints.

The noise factor is used to measure the degradation of the SNR and the lower the value of the noise factor, the better the receiver performance. According to the Friis formula (FRIIS, 1944), the receiver sensitivity depends mainly on the first RF block. In this regard, the receiver circuit designer works with a special focus on optimizing the LNA noise factor, since it directly affects the receiver sensitivity. Hence, the overall noise factor can be expressed as

$$\begin{aligned} F_{j,\mathrm{mode}} &= F_{\mathrm{LNA,mode}} + \frac{F_{\mathrm{SubsequentBlocks}} - 1}{G_{\mathrm{LNA,mode}}} \\ &\approx F_{\mathrm{LNA,mode}}, \end{aligned} \tag{3.1}$$

where $F_{\mathrm{SubsequentBlocks}}$ is the combined noise factor of the subsequent blocks at the receiver chain, while $F_{\mathrm{LNA,mode}}$ and $G_{\mathrm{LNA,mode}}$ are the noise factor and the linear voltage gain of the LNA, respectively, which depend on its respective operating mode. Table 3.2 summarizes the LNA measured performance for its three operating modes. As we can note, since the LNA gain is high ($G_{\mathrm{LNA}} \geq 16.8$ dB), the receiver noise factor can be well approximated by the LNA noise factor. Also, note that the LNA can save power from $1.5\times$ to $3\times$.

Table 3.2: Characteristics of the proposed LNA for each operating mode at 2.4 GHz.

Operating Mode	Voltage Gain ($G_{\mathrm{LNA,mode}}$) [dB]	Noise Factor ($F_{\mathrm{LNA,mode}}$)	Power Consumption ($P_{\mathrm{LNA},j,\mathrm{mode}}$) [mW]
1	16.8	5.4	0.3
2	18.8	4.7	0.6
3	21.5	4.3	0.9

It is worth noting that in the case of cooperative communication, we assume that the LNAs of all relay nodes operate in the same mode during the broadcast phase.

[2]Let us note that the noise factor (F) is linear and the noise figure (NF) is expressed in decibels (dB).

3.3 Communication System Model

In this section, we present the mathematical model that represents the transmission of information over the wireless channel, including the reconfigurable parameters of the amplifiers, that is, the output power of the PA and the noise factor of the LNA. In addition, to represent the fading of the wireless channel, we adopt the Rayleigh distribution, which is normally used in cases where there is non-line-of-sight (NLOS) between communicating nodes. Then, omitting the time index, the source message received by the node j after a transmission performed by the node i can be represented in the form

$$\mathbf{y}_{ij} = \sqrt{\frac{\kappa_{ij}\, P_{i,\mathrm{mode}}}{n_i}}\, \mathbf{H}_{ij}\, \mathbf{x}_{ij} + \mathbf{w}_{ij}, \tag{3.2}$$

where $\mathbf{y}_{ij} \in \mathbb{C}^{n_j \times 1}$ is the received signal vector, κ_{ij} is the link budget relationship in the i-j link, $P_{i,\mathrm{mode}}$ is the PA transmission power distributed per active antenna n_i, $\mathbf{H}_{ij} \in \mathbb{C}^{n_j \times n_i}$ is the matrix of quasi-static channel coefficients, whose elements $h_{ij} \in \mathbf{H}_{ij}$ are independent and identically distributed random variables with zero-mean and unit-variance Rayleigh distribution. In addition, $\mathbf{x}_{ij} \in \mathbb{C}^{n_i \times 1}$ is the unit energy transmitted symbol vector and $\mathbf{w}_{ij} \in \mathbb{C}^{n_j \times 1}$ is the additive white Gaussian noise (AWGN) vector, with variance $N_0/2$ per dimension, where N_0 is the unilateral thermal noise power spectral density.

The link budget relationship is assumed to be (GOLDSMITH, 2005)

$$\kappa_{ij} = \frac{A\,\lambda^2}{L\,(4\pi)^2\,(d_{ij})^{\alpha}}, \tag{3.3}$$

where A is the total antenna gains, $\lambda = \frac{3.10^8}{f_\mathrm{c}}$ is the wavelength, f_c is the carrier frequency, L is the link margin, d_{ij} is the distance between communicating nodes and α is the path loss exponent.

Moreover, the instantaneous SNR at the receiver j after a transmission from i is

$$\gamma_{ij} = \|\mathbf{H}\|_F^2 \cdot \bar{\gamma}_{ij}, \tag{3.4}$$

where $\|.\|_F$ is the Frobenius norm and the average SNR at each receive antenna with respect to each transmit antenna is then measured as

$$\bar{\gamma}_{ij} = \frac{P_j}{F_{j,\mathrm{mode}}\, N}, \tag{3.5}$$

in which $P_j = \frac{\kappa_{ij}\, P_{i,\mathrm{mode}}}{n_i}$ is the received power, $F_{j,\mathrm{mode}}$ is the noise factor of the LNA and $N = N_0\, B$ is the noise power, where B is the system bandwidth.

3.4 Summary of the Chapter

Nowadays, with different operating requirements for wireless communication systems, reconfigurable RF transceivers have become an interesting solution, since employing multi-chips into a device can increase the cost, size and power consumption. As detailed in Sections 3.1 and 3.2, the reconfigurable amplifier designs feature different operating modes for performance and energy consumption, making it a crucial venue to perform different IoT applications. It is worth mentioning that we exploit the features of only one reconfigurable circuit in the transmitter and receiver chain; however, other building blocks of the RF transceiver can also be included in the system model.

For our EE analysis, we model the system level design in Section 3.3 with the PA transmission power and the LNA noise factor. It is important to note that the operating modes of the PA and LNA circuits directly impact the average SNR at the receiver. Hence, the properly adaptation of these circuits affects the EE of the communication system, as it will be discussed in the following chapters. More specifically, Chapter 4 focuses on non-cooperative MIMO schemes with SE optimization for the EE analysis, while Chapter 5 encompasses cooperative SISO nodes with multiple relays.

CHAPTER 4

NON-COOPERATIVE MULTIPLE ANTENNA SCHEMES

Let us take on the MIMO system depicted in Fig. 4.1, for which two transmission schemes are considered: Fig. 4.1a based on AS, in which a single pair of antennas is activated at the source and destination, requiring a single RF chain at each side; and Fig. 4.1b MIMO beamforming scheme based on SVD, which uses precoding and equalization techniques in order to improve reliability by using all transmit and receive antennas. Further, the SISO scheme is also considered for comparison. First, we present two metrics for these transmission schemes, the outage probability and the EE. Next, we elaborate the EE optimization problem and demonstrate the algorithm used for the simulations. After that, we show some numerical examples to evaluate the EE for the schemes under test and, finally, we summarize the main results obtained.

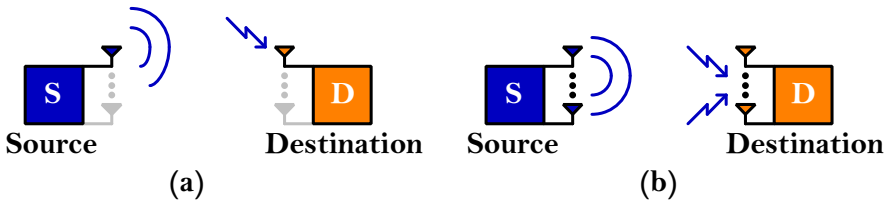

Figure 4.1: Non-cooperative MIMO system: (a) AS scheme and (b) SVD scheme.

4.1 Single Antenna (SISO)

In the SISO scheme, where the source and destination nodes are equipped with a single antenna ($n_{\mathrm{S}} = n_{\mathrm{D}} = 1$), the mutual information is defined as (GOLDSMITH, 2005)

$$I_{\mathrm{SISO}} = B \, \log_2 \left(1 + \gamma_{\mathrm{SD}}\right), \tag{4.1}$$

where $\gamma_{\mathrm{SD}} = \bar{\gamma}_{\mathrm{SD}} \cdot |h_{\mathrm{SD}}|^2$ and an outage event occurs whenever I_{SISO} falls below the information rate $R_{\mathrm{b}} = \xi \cdot B$, where ξ is the spectral efficiency in bps/Hz. Then, assuming the Rayleigh

distribution, in which $|h_{\mathrm{SD}}|^2$ has an exponential distribution, the outage probability of SISO is given by (GOLDSMITH, 2005)

$$\begin{aligned}\mathcal{O}_{\mathrm{SISO}} &= \Pr\left\{I_{\mathrm{SISO}} < R_{\mathrm{b}}\right\} \\ &= \Pr\left\{|h_{\mathrm{SD}}|^2 < \frac{2^{\xi}-1}{\bar{\gamma}_{\mathrm{SD}}}\right\} \\ &= 1 - \exp\left(-\frac{2^{\xi}-1}{\bar{\gamma}_{\mathrm{SD}}}\right).\end{aligned} \tag{4.2}$$

Another important metric is the system throughput, defined as the rate of correct information transfer between the source and the destination, as follows

$$\mathcal{T}_{\mathrm{SISO}} = \xi \cdot \left(1 - \mathcal{O}_{\mathrm{SISO}}\right), \tag{4.3}$$

in which the destination receives ξ bps/Hz if the transmission from the source is successful.

When calculating the EE, it is necessary to take into account the total power consumption that includes the transmission power and the power consumed by the RF circuits. Let us remark that, as this work targets narrowband applications with a single frequency carrier, the portion of power that is consumed by baseband processing has been ignored. However, it is worth mentioning that in multi-carrier broadband transceivers, the baseband consumption can be compatible with that of RF circuits (BOUGARD et al., 2007). Next, we define the EE of the SISO in bps/Hz/W or equivalently in bits/J/Hz as

$$\eta_{\mathrm{SISO}} = \xi \cdot \frac{\left(1 - \mathcal{O}_{\mathrm{SISO}}\right)}{P_{\mathrm{PA,S,mode}} + P_{\mathrm{TX,S}} + P_{\mathrm{LNA,D,mode}} + P_{\mathrm{RX,D}}}. \tag{4.4}$$

Therefore, in order to maximize EE, the power consumed by the RF transceiver must be minimized. That is, reconfigurable circuits can help achieving this goal.

4.2 Antenna Selection (AS)

Since increasing the number of antennas can increase the power consumption, then the AS technique may be of particular interest to reduce the number of RF chains. In the case of AS, a single RF chain will be active at the source and destination nodes, *i.e.*, $n_{\mathrm{S}} = 1$ out of N_{S} antennas is selected at the source and $n_{\mathrm{D}} = 1$ out of N_{D} antennas is selected at the destination. We assume that the best pair of antennas can be chosen by the destination during the transmission of pilot symbols prior to each frame. Then, the destination informs the best transmit antenna (using only a few bits) via feedback channel. Thus, once the pair of antennas is activated in order to maximize the SNR, the mutual information of the AS scheme becomes

$$I_{\mathrm{AS}} = B \, \log_2 \left(1 + \bar{\gamma}_{\mathrm{SD}} \cdot \max_{k,l} |h_{\mathrm{SD},k,l}|^2 \right), \tag{4.5}$$

where k belongs to the set of antennas at the transmitter and l is the equivalent at the receiver, so that the outage probability of AS follows (BRANTE et al., 2013)

$$\mathcal{O}_{\mathrm{AS}} = \left[1 - \exp\left(-\frac{2^{\xi} - 1}{\bar{\gamma}_{\mathrm{SD}}} \right) \right]^{N_{\mathrm{S}} \, N_{\mathrm{D}}}. \tag{4.6}$$

Moreover, as only one antenna is active at each node, the EE of the AS scheme is

$$\eta_{\mathrm{AS}} = \xi \cdot \frac{(1 - \mathcal{O}_{\mathrm{AS}})}{P_{\mathrm{PA,S,mode}} + P_{\mathrm{TX,S}} + P_{\mathrm{LNA,D,mode}} + P_{\mathrm{RX,D}}}, \tag{4.7}$$

where, we remark that although (4.7) is very similar to (4.4), the outage probability of AS is lower than that of SISO, due to the exponent $N_{\mathrm{S}} \, N_{\mathrm{D}}$ in (4.6), while the power consumption is similar, once a single RF chain is active at each side in both schemes. Thus, it is expected that AS yields a higher EE than SISO.

4.3 Singular Value Decomposition (SVD) Beamforming

The use of beamforming through the SVD technique allows to exploit all $n_{\mathrm{S}} = N_{\mathrm{S}}$ and $n_{\mathrm{D}} = N_{\mathrm{D}}$ antennas at once, ergo the mutual information of the SVD scheme can be expressed as (TSE; VISWANATH, 2005)

$$\begin{aligned} I_{\mathrm{SVD}} &= B\,\log_2\left[\det\left(\mathbf{I}_n + \bar{\gamma}_{\mathrm{SD}}\cdot\mathbf{H}_{\mathrm{SD}}\,\mathbf{H}_{\mathrm{SD}}^{\dagger}\right)\right], \\ &= B\sum_{l=1}^{n}\log_2\left(1+\bar{\gamma}_{\mathrm{SD}}\cdot\lambda_l^2\right), \end{aligned} \tag{4.8}$$

where $\mathbf{I}_n$ is an identity matrix, with $n = \min\{N_{\mathrm{S}}, N_{\mathrm{D}}\}$, † denotes the conjugate transpose operation and λ_l are the eigenvalues of $\mathbf{H}_{\mathrm{SD}}\,\mathbf{H}_{\mathrm{SD}}^{\dagger}$. In addition, by using Jensen's inequality, the mutual information of SVD can be upper bounded by (TSE; VISWANATH, 2005)

$$\frac{1}{n}\sum_{l=1}^{n}\log_2\left(1+\bar{\gamma}_{\mathrm{SD}}\cdot\lambda_l^2\right) \leq \log_2\left(1+\frac{\bar{\gamma}_{\mathrm{SD}}}{n}\sum_{l=1}^{n}\lambda_l^2\right), \tag{4.9}$$

and since $\sum_{l=1}^{n}\lambda_l^2 = \mathrm{Tr}\left(\mathbf{H}_{\mathrm{SD}}\mathbf{H}_{\mathrm{SD}}^{\dagger}\right) = \sum_{k,l}|h_{\mathrm{SD},k,l}|^2$, then the outage probability of SVD becomes (BRANTE et al., 2013)

$$\mathcal{O}_{\mathrm{SVD}} \geq 1-\exp\left(-\frac{\rho}{\bar{\gamma}_{\mathrm{SD}}}\right)\sum_{m=0}^{N_{\mathrm{S}}\,N_{\mathrm{D}}-1}\frac{1}{m!}\left(\frac{\rho}{\bar{\gamma}_{\mathrm{SD}}}\right)^{m}, \tag{4.10}$$

where $\rho = n\,\left(2^{\xi/n}-1\right)$.

It is worth noting that SVD requires a feedback channel with large capacity, which may not be very practical. On the other hand, AS requires only a few bits of feedback, needed to inform the antenna index. However, our goal when comparing SVD with AS is to provide a benchmark in terms of energy efficiency[1].

[1]Let us remark that, as our numerical results will show, even neglecting the energy consumption of the feedback channel of SVD, and considering a lower bound for the outage probability in (4.10), AS still outperforms SVD in most situations.

Finally, the EE of SVD is then calculated as

$$\eta_{\mathrm{SVD}} \leq \xi \cdot \frac{(1-\mathcal{O}_{\mathrm{SVD}})}{N_{\mathrm{S}}\left(P_{\mathrm{PA,S,mode}}+P_{\mathrm{TX,S}}\right)+N_{\mathrm{D}}\left(P_{\mathrm{LNA,D,mode}}+P_{\mathrm{RX,D}}\right)}. \tag{4.11}$$

It is worth mentioning that, as the frequency synthesizer circuit can be shared among all the antenna paths (CUI; GOLDSMITH; BAHAI, 2004), then we assume only one frequency synthesizer at the transmitter side and one for the receiver.

Furthermore, once the mutual information of SVD is higher than that of AS and SISO (TSE; VISWANATH, 2005), it yields the highest throughput compared to the other schemes. On the other hand, since all RF chains are active, the power consumption is also higher, which may present a few trade-offs in terms of EE compared to SISO and AS. In addition, let us remark that the EE in (4.11) is an optimistic result, since the outage probability of SVD is lower bounded in our analysis.

4.4 Optimization Problem

In order to maximize the EE of the communication system, we aim at a joint selection of the best operating modes for the PA and LNA circuits. Let us remark that the operating mode of the PA dictates the employed transmission power, while the operating mode of the LNA modifies the sensitivity of the receiver. Besides, we also assume that the SE can be proper adjusted by changing modulation and coding at the transmitter. So that, we use $\mathrm{PAPR} = 3\,(\sqrt{M}-1)/(\sqrt{M}+1)$, given by (CUI; GOLDSMITH; BAHAI, 2005). Note that M is the constellation size of the M-ary quadrature amplitude modulation (QAM) scheme, which depends on the SE value ($M = 2^{\xi}$). It is important to note that the PAPR is equal to 0 dB when $\xi = 2$. However, in the case of SE values $\xi > 2$, we consider that the PA operates at different backed-off power levels. In other words, the higher the SE value, the higher the throughput and the lower the transmission power at the PA output. Moreover, we also consider different antenna arrangements $(N_{\mathrm{S}} = N_{\mathrm{D}}) \geq 2$. It is worth mentioning that we consider $N_{\mathrm{S}} = N_{\mathrm{D}}$ based on an IoT network, in which the transmitting and receiving nodes have the same hardware. However,

the analysis can be extended to arbitrary values of N_{S} and N_{D}. Thus, our optimization problem becomes

$$\begin{aligned} \max_{P_{\mathrm{S,mode}},\, F_{\mathrm{D,mode}},\, \xi} \quad & \eta_{(\mathrm{sch})} \rightarrow \mathrm{sch} \in \{\mathrm{AS}, \mathrm{SVD}\}, \\ \text{s.t.} \quad & P_{\mathrm{S,mode}} \in \mathcal{S}_{\mathrm{PA}}, \\ & F_{\mathrm{D,mode}} \in \mathcal{S}_{\mathrm{LNA}}, \\ & \xi \geq 2, \\ & \mathcal{O}_{(\mathrm{sch})} \leq \mathcal{O}^{\star}, \end{aligned} \tag{4.12}$$

where $\mathcal{S}_{\mathrm{PA}}$ is the set of transmission powers provided by the 9 operating modes of the PA, according to Table 3.1 and $\mathcal{S}_{\mathrm{LNA}}$ is the set of the noise factors yielded by the 3 operating modes of the LNA, according to Table 3.2. While $\mathcal{O}^{\star}$ represents the target outage probability at the receiver.

Algorithm 1 details the employed approach in order to jointly optimize $P_{\mathrm{S,mode}}$, $F_{\mathrm{D,mode}}$ and ξ. Due to the limited solution space, we resort to an exhaustive search to solve the optimization problem in (4.12), in which $\mathcal{S}_{\xi}$ is the set of available spectral efficiencies. Notice that this set depends on the particular employed RF transceiver, as it is a functon of the available choices for modulation and code rates. Moreover, $P_{\mathrm{S,mode}}$ and $F_{\mathrm{D,mode}}$ also belong to discrete sets. Then, a look-up table (LUT) can be easily implemented in practice, with the size of the LUT being $|\mathcal{S}_{\mathrm{PA}}| \times |\mathcal{S}_{\mathrm{LNA}}| \times |\mathcal{S}_{\xi}|$, where $|\cdot|$ represents the cardinality of the set. Thus, $27 \times |\mathcal{S}_{\xi}|$ entries for the LUT are required in our problem, in which we consider a large set for $\mathcal{S}_{\xi}$ in our simulations. However, $|\mathcal{S}_{\xi}|$ may be quite small in practice, so that the complexity of the proposed solution is small.

Furthermore, we also assume that the adaptation of the PA and LNA operating modes is done during the transmission of pilot symbols prior to each frame. Let us remark that the pilot symbols exchange is already required for channel estimation due to the MIMO transmission schemes. As a consequence, only a few aditional bits are required, depending on the number of available modes.

Algorithm 1 EE maximization for each transmission $\mathrm{sch} \in \{\mathrm{AS}, \mathrm{SVD}\}$.

Input: d_{SD}, $\mathcal{O}^{\star}$

$index \leftarrow 1$; $\eta_{(\mathrm{sch}),index-1} \leftarrow 0$
for $\xi \in \mathcal{S}_{\xi}$ **do**
  for $P_{\mathrm{S,mode}} \in \mathcal{S}_{\mathrm{PA}}$ **do**
    for $F_{\mathrm{D,mode}} \in \mathcal{S}_{\mathrm{LNA}}$ **do**
      ; compute $[P_{\mathrm{S,mode}} - \mathrm{PAPR}(\xi)] \rightarrow$ in [dB]
      ; compute $F_{\mathrm{D,mode}}$ using (3.1)
      ; compute $P_{\mathrm{PA,S,mode}}$ and $P_{\mathrm{LNA,D,mode}}$
      ; compute κ_{SD} and $\bar{\gamma}_{\mathrm{SD}}$ using (3.3) and (3.5)
      ; compute $\mathcal{O}_{(\mathrm{sch})}$ using (4.2), (4.6) and (4.10)
      if $\mathcal{O}_{(\mathrm{sch})} > \mathcal{O}^{\star}$ **then**
        $\eta_{(\mathrm{sch}),index} \leftarrow 0$
      else
        ; compute $\eta_{(\mathrm{sch}),index}$ using (4.4), (4.7) and (4.11)
        if $\eta_{(\mathrm{sch}),index} < \eta_{(\mathrm{sch}),index-1}$ **then**
          $\eta_{(\mathrm{sch}),index} \leftarrow \eta_{(\mathrm{sch}),index-1}$
        end if
      end if
    end for
  end for
end for

Output: $\eta_{(\mathrm{sch}),index}$

4.5 Numerical Results

In this section, we evaluate the EE numerically in different transmission scenarios considering our proposed optimization approach. The EE results were obtained through simulations performed in the MATLAB® computational environment. Table 4.1 describes the parameters used in the simulations.

Moreover, we compare the performance of the reconfigurable PA and LNA described in Sections 3.1 and 3.2, respectively, with two state-of-the-art non-reconfigurable designs that are among the best figures of merit found in the literature so far. The chosen PA and LNA used for comparison aim at high-performance. In other words, their design focus on good performance in terms of high output power for the PA and low noise factor for the LNA, rather than having reconfigurable capabilities. We employ the PA proposed by (HAYATI; SHEIKHI; GREBENNIKOV, 2015), which consumes 246.8 mW at 2.4 GHz, yielding an output power of 23.6 dBm. Whereas the LNA proposed by (PATHAK et al., 2020) provides a noise factor of 2.3,

Table 4.1: System parameters for MIMO communication.

Parameter	Description	Value
B	bandwidth	180 kHz †
L	link margin	20 dB
f_{c}	carrier frequency	2.4 GHz
A	total antenna gain	5 dBi ‡
α	path loss exponent	2.5 ‡
$\mathcal{O}^{\star}$	target outage probability	10^{-3} ‡
N_0	noise power spectral density	-174 dBm/Hz ‡
$P_{\mathrm{TX,S}}$	non-reconf. TX power consumption	98 mW ‡
$P_{\mathrm{RX,D}}$	non-reconf. RX power consumption	94.4 mW ‡

†Source: (3GPP TR 36.888, 2013),
‡Source: (NAEEM; PATWARY; ABDEL-MAGUID, 2017).

besides to a gain of 24 dB and occupies the frequency range between 2.2 GHz and 2.55 GHz, with a power consumption of 0.957 mW.

4.5.1 Energy Efficiency with Fixed Spectral Efficiency

First, let us consider the case when the optimization problem in (4.12) is solved with fixed SE, *i.e.*, only the effect of the PA and LNA operating modes are considered. In the Fig. 4.2, we plot the EE of SISO, AS and SVD schemes as a function of the distance when $N_{\mathrm{S}} = N_{\mathrm{D}} = 2$ antennas and $\xi = 2$ bps/Hz, which corresponds to a PAPR = 0 dB. The goal here is to show the transmission range for each operating mode of the PA. First, note that the curves appear to be incomplete, since each scheme can only transmit up to a given range due to the QoS constraint ($\mathcal{O}_{(\mathrm{sch})} \leq \mathcal{O}^{\star}$). Further, we can see that mode 1 (low-power) is the most energy-efficient due to the lowest-power consumption, while mode 9 (high-performance) allows to reach longer distances with the penalty of EE. We also note that the EE of SISO and AS is higher for short-range communications, but the distance range of AS is greater than that of SISO. Due to the lower outage probability, SVD performs longer transmissions than other schemes; however, let us remark that this scheme consumes more power at the circuit level, which impacts on EE.

In Fig. 4.3, we provide a comparison between reconfigurable and non-reconfigurable designs. For the curves of reconfigurable designs, we observe that AS outperforms the other

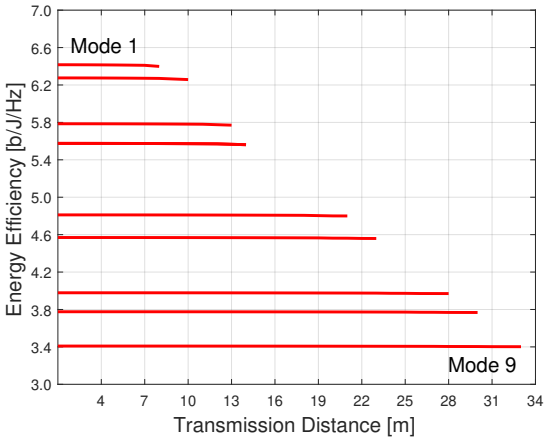

(a) SISO.

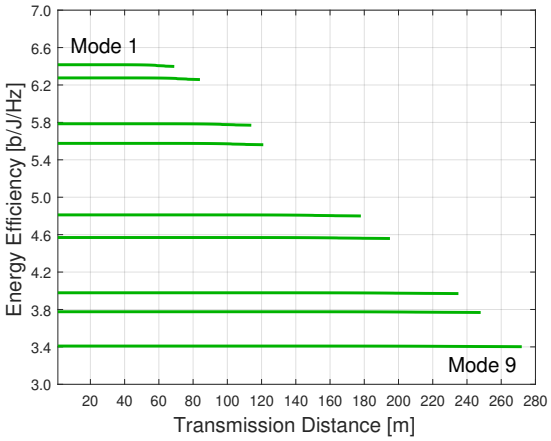

(b) AS.

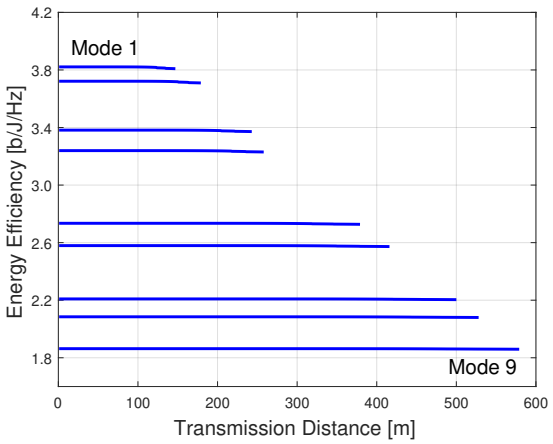

(c) SVD.

Figure 4.2: EE of SISO, AS and SVD schemes for each PA operating mode with reconfigurable LNA, when $\xi = 2$ bps/Hz and $N_{\mathrm{S}} = N_{\mathrm{D}} = 2$ antennas.

schemes in terms of EE, but SVD allows longer communication distances, which may be important to some IoT applications. In addition, for short-range communications, the EE obtained using the reconfigurable circuits is significantly higher compared to the non-reconfigurable circuits. For instance, at distances up to 67 meters, an energy gain above 49% for SVD and 40% for AS is achieved, while for SISO we observe an improvement in distances of up to 23 meters. As a conclusion, to significantly reduce the energy required an end-to-end communication, the proposed approach shows that the design and development of reconfigurable RF circuits is crucial towards improving the EE of modern applications, which have very distinct communication ranges. Besides that, we also observe that the performance using non-reconfigurable circuits becomes better at longer distances. Such behavior occurs since the circuits from (HAYATI;

SHEIKHI; GREBENNIKOV, 2015; PATHAK et al., 2020), as most of the approaches for the constructions of PAs and LNAs, are designed for these operating points. Thus, these circuits can be optimized for long distances, sacrificing reconfigurability. To compare, the PA from (HAYATI; SHEIKHI; GREBENNIKOV, 2015) provides a transmission power of 23.6 dBm, while the mode 9 of the PA from Section 3.1 yields 16.9 dBm. In addition, the LNA noise factor from (PATHAK et al., 2020) is 2.3, while the mode 3 of the LNA from Section 3.2 has a noise factor of 4.3.

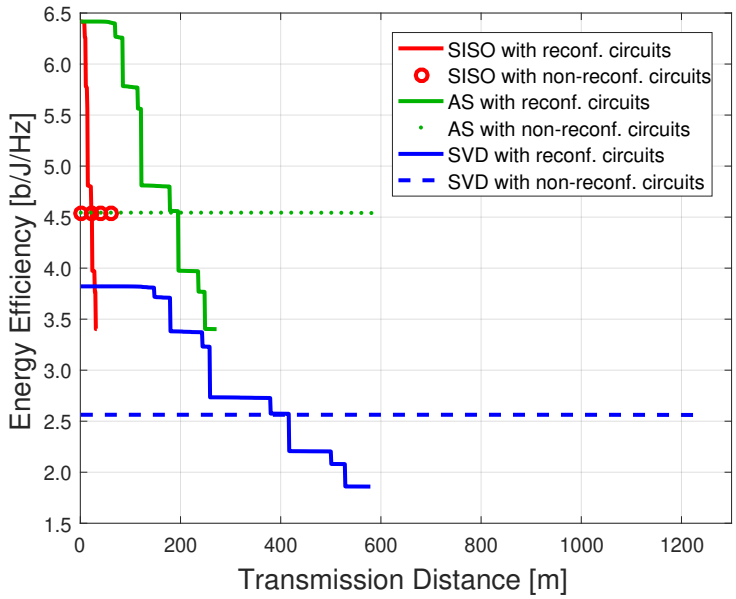

Figure 4.3: EE of SISO, AS and SVD, comparing reconfigurable and non-reconfigurable circuits, when $\xi = 2$ bps/Hz and $N_{\mathrm{S}} = N_{\mathrm{D}} = 2$ antennas.

Fig. 4.4 complements the analysis, showing the total power consumption of SISO, AS and SVD schemes, represented by the black dashed lines and the axis on the left side of the figure. In addition, the operating mode of the PA and LNA circuits are also shown as a function of the distance, represented by the colored bars and the axis on the right side of the figure. So, a first observation shows that the reconfigurable LNA switches its operating mode before the reconfigurable PA, which is expected since its consumption is lower when compared to the PA. That is, the PA remains in the lowest-power consumption point (mode 1) as much as possible, while the LNA switches its operating mode with the increase of the distance in order to improve the sensitivity at the receiver. When it is not possible to improve the sensitivity even further by changing the LNA operating mode, then the PA operating mode changes to increase the

transmission power. After the PA switches its operating mode, we observe that the LNA returns to a lower operating mode in order to adjust the RF signal gain at the receiver. Furthermore, we can also conclude that the power consumption of AS is similar to that of SISO, whereas SVD consumes considerably more power at the circuit level.

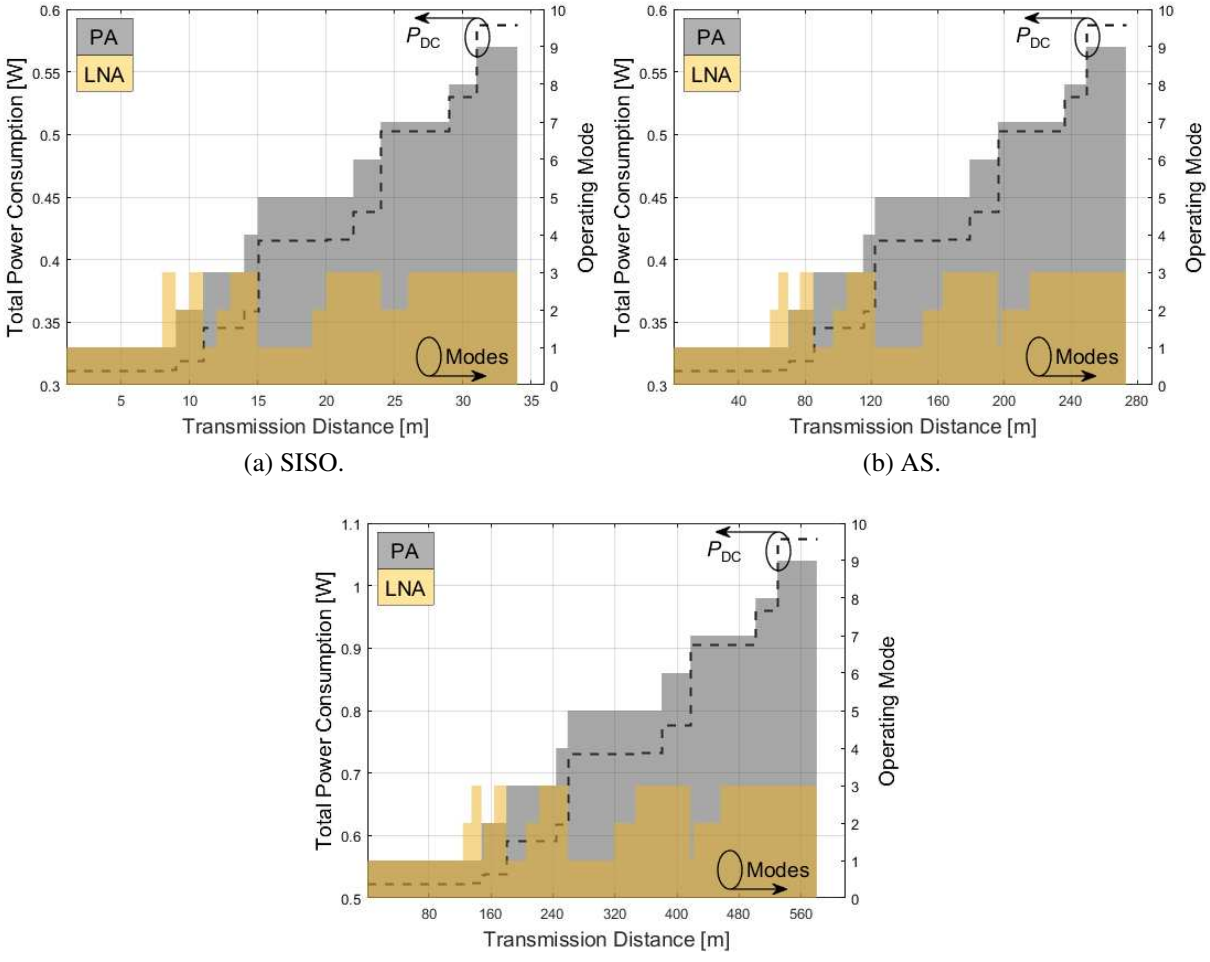

(a) SISO.

(b) AS.

(c) SVD.

Figure 4.4: Overall power consumption and best operating mode for the PA and LNA circuits, of SISO and MIMO schemes, when $\xi = 2$ bps/Hz and $N_{\mathrm{S}} = N_{\mathrm{D}} = 2$ antennas.

4.5.2 Energy Efficiency with Optimized Spectral Efficiency

Hereafter, we optimize the SE along with the PA and LNA operating modes in order to maximize the EE. First, Fig. 4.5 depicts the EE as a function of the SE with $\mathcal{S}_{\xi} \in [2, 16]$ for two link distances between the source and the destination. From the figure, we observe that the SE contributes to maximize the EE. That is, at a certain communication distance, there is an

optimum SE value that maximizes each transmission scheme. Moreover, the optimum SE value for each scheme as a function of the distance is shown in Fig. 4.6. As we observe, the RF signal is transmitted with high SE for short-range communications, since the communication channel has higher SNR. However, when the distance increases, notice that the SE decreases to meet the target outage probability at the receiver.

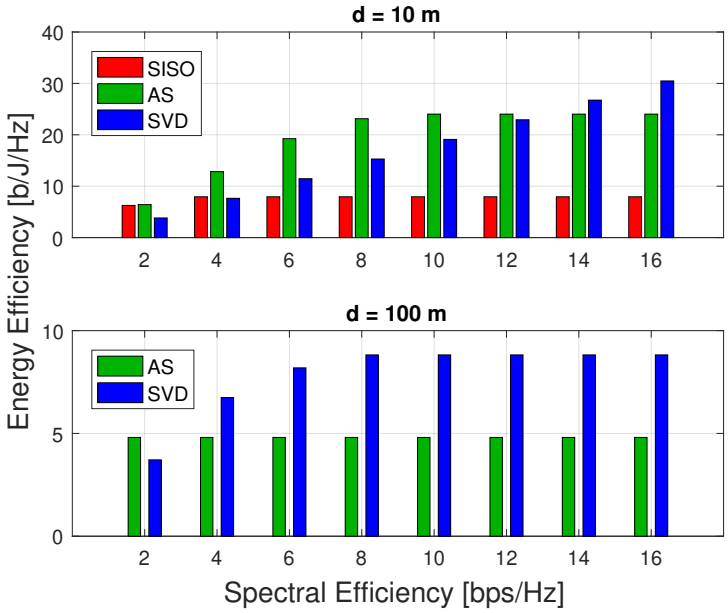

Figure 4.5: EE versus SE, when $N_{\mathrm{S}} = N_{\mathrm{D}} = 2$ antennas.

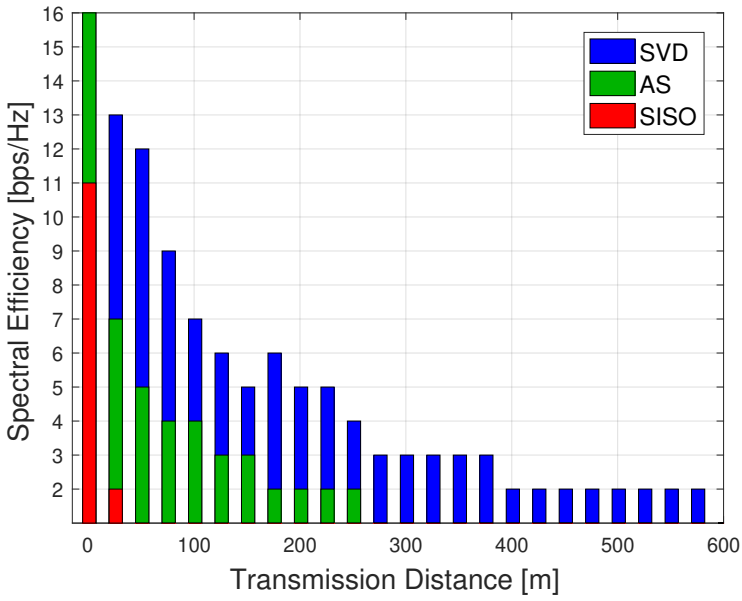

Figure 4.6: Optimum SE as a function of the distance, when $N_{\mathrm{S}} = N_{\mathrm{D}} = 2$ antennas.

Fig. 4.7 illustrates the EE of SISO and MIMO schemes. First, we can see an 'oscillation' in the EE curve that reflects the switching of the PA and LNA operating modes along with the SE optimization. Next, comparing with Fig. 4.3, we observe a significant gain in terms of EE. In addition, the AS is still more energy-efficient than SISO; however, the EE of AS remains higher than that of SVD only for very short distances. More interestingly, we can notice that when optimizing the SE, the SVD scheme became more energy-efficient than SISO and, therefore, compensating the issue of circuitry power consumption that would impact the EE for short distances. Furthermore, it is worth mentioning that we use very high spectral efficiencies in this analysis for the sake of illustration; however, in practice this will be limited by the available modulation and coding at the transmitter.

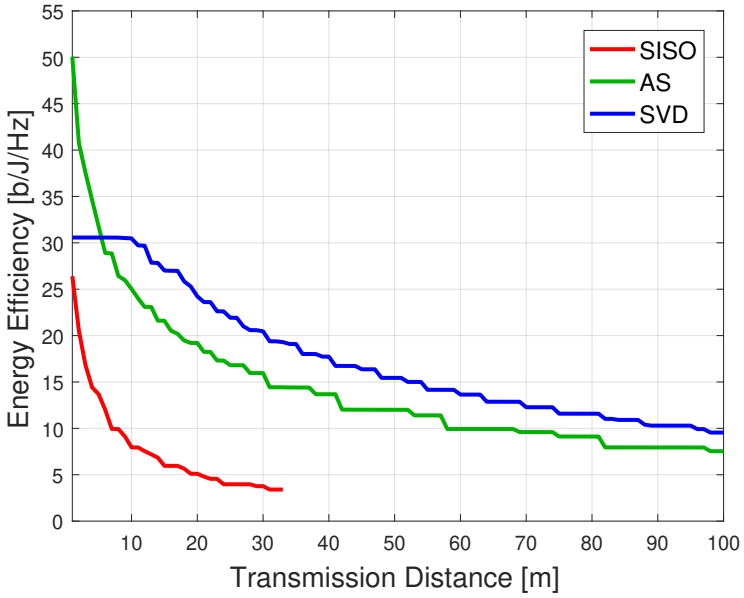

Figure 4.7: EE of SISO, AS and SVD schemes with the joint optimization of the PA and LNA operating modes, as well as the SE, when $N_{\mathrm{S}} = N_{\mathrm{D}} = 2$ antennas.

Fig. 4.8 depicts the selected operating modes for the PA and LNA circuits as a function of the distance, as well as the total power consumption. Compared to Fig. 4.4, where the total power consumption is a non-decreasing function of the transmission distance, here the total power consumption oscillates a bit more since the PA changes its operating modes more constantly. Such interesting behavior can be explained by the reconfiguration of SE in order to maintain an acceptable communication quality given by the target outage. Furthermore, it is noteworthy that optimizing the SE does not decrease the power consumption at the circuit level,

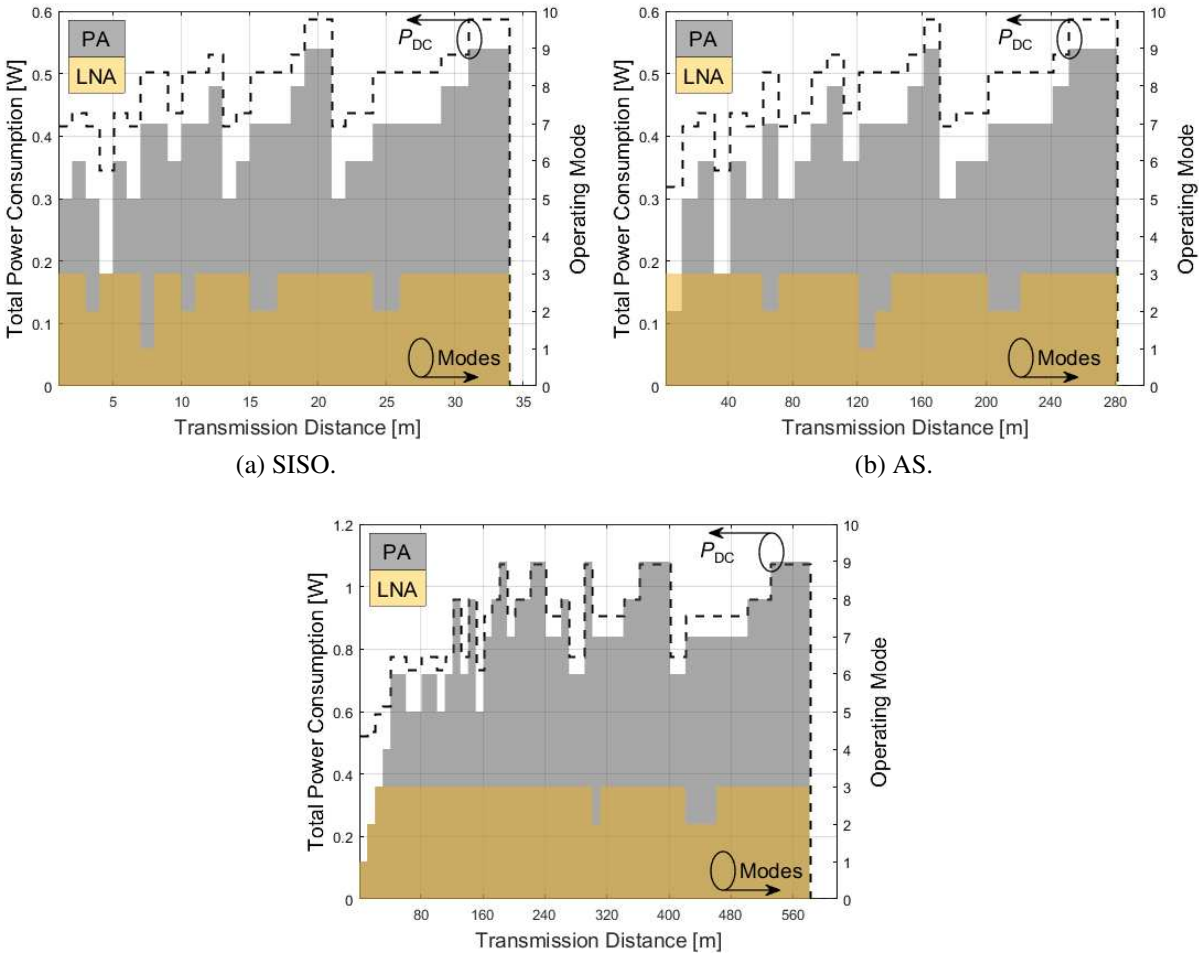

(a) SISO.

(b) AS.

(c) SVD.

Figure 4.8: Overall power consumption and best operating mode for the PA and LNA circuits, when optimizing the SE with $N_{\mathrm{S}} = N_{\mathrm{D}} = 2$ antennas.

but increases the system throughput which impacts the EE. Therefore, depending on the SE, the reconfigurable RF amplifiers adapt their operating modes in order to enhance the EE.

4.5.3 Considerations About Optimizing the Number of Antennas

In this subsection, we aim to provide some insights on how the number of antennas affects the EE performance. First, Fig. 4.9 evaluates the EE as a function of the number of antennas, which we consider to be the same in both source and destination nodes, *i.e.*, $N_{\mathrm{S}} = N_{\mathrm{D}}$. Moreover, we also consider the optimization of the PA and LNA operating modes, as well as the SE. Considering the communication distances under analysis 100 m and 250 m, we note that when we increase the number of antennas, AS achieves higher EE, but the EE gain increases slowly

after a certain number of antennas. In the case of SVD, there is an optimum number of antennas with the reconfigurable approach that maximizes the EE. In our examples, 4×4 antennas is optimal for $d = 100$ m, while a 5×5 arrangement is optimal for $d = 250$ m.

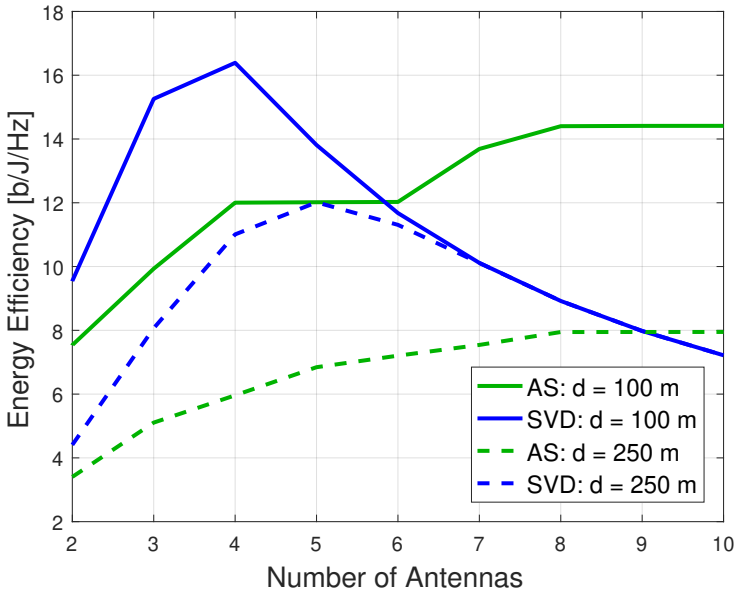

Figure 4.9: EE versus number of antennas with $N_{\mathrm{S}} = N_{\mathrm{D}}$.

Therefore, the optimization of the number of active antennas in SVD would be another interesting approach. In order to illustrate that, we consider in Fig. 4.10 that the SVD scheme can randomly choose $n^{\star}$ out of $N_{\mathrm{S}} = N_{\mathrm{D}}$ antennas, while we restrict the search space for $N_{\mathrm{S}} = N_{\mathrm{D}} \in [2, 10]$ as an example. In Fig. 4.10a, note that the optimum number of antennas relies on the communication distance, which is an important issue to be considered in the EE analysis, as shown in Fig. 4.9. Thus, Fig. 4.10b plots the EE as a function of the transmission distance, including the additional optimization of $n^{\star}$ for the SVD scheme. From the Fig. 4.10b, we can see not only an increase in the EE, but also an increase in the communication distance, showing that our approach has a significant impact for future deployments of MIMO systems. Let us also remark that such approach can be further optimized in order to choose the $n^{\star}$ best antennas out of $N_{\mathrm{S}} = N_{\mathrm{D}}$, *i.e.*, by selecting the $n^{\star}$ antennas that yield the lower outage probability, or the higher EE. However, this implies in re-calculating the outage probability to take into account the additional spatial diversity, which we leave for future investigations.

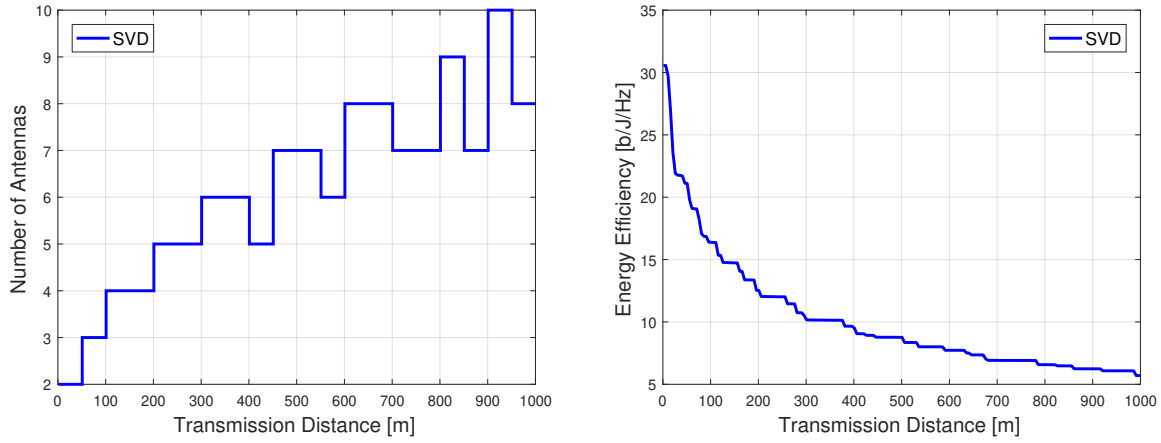

(a) (b)

Figure 4.10: (a) Optimum number of antennas for the SVD scheme; (b) EE of SVD with the joint optimization of the PA and LNA operating modes, the SE and the number of antennas.

4.6 Summary of the Chapter

In this chapter, the performance of the SISO, AS and SVD schemes in terms of EE is compared. In our optimization problem, we propose the joint selection of the best operating mode for the PA and LNA circuits, in addition to optimizing the SE. It was found that the AS technique allows to save energy, in which the results show that it perform better over short distances for all evaluated scenarios. However, there are conditions in which the SVD becomes more energy-efficient, reaching even longer communication distances in relation to the other schemes.

In our first analysis, we evaluate the EE taking into account only the reconfigurability of the PA and LNA circuits, then we fix the SE and the number of antennas. In this scenario, we illustrate the EE and the transmission for each PA operating mode with the reconfigurable LNA, and the results show that the low-power mode achieves the highest EE, while the longest transmission distance is achieved by switching to the highest-performance mode. In addition, we conduct a comparison with circuits that were designed for performance with a fixed operating point. In this case, the results show that reconfigurable circuits are of paramount importance towards improving the EE; however, it is worth mentioning that with the penalty of EE, non-reconfigurable circuits reach longer distances compared to reconfigurable circuits. Also, we

complement that in very short transmissions, the SISO is more energy-efficient than the SVD scheme, as each antenna added to the SVD increases the power consumption.

Then, by reconfiguring the SE with the RF amplifier circuits, the results show a significant increase in the EE for all transmission schemes, that is, there is an optimum value of SE that maximizes the EE. Over short distances, it has been noticed that MIMO systems improve their performance with higher spectral efficiencies. Furthermore, in this scenario, the SVD becomes more energy-efficient than the SISO and, more significantly, in less than 10 meters the SVD outperformed the AS scheme.

Finally, we also considered optimizing the number of antennas. That is, we indicate that different antenna arrangements corroborate to enhance the EE. So, the joint optimization of the PA and LNA operating modes, SE and number of antennas stands out as a promissing solution to maximize the EE, which still requires a thorough investigation in the future.

CHAPTER 5

INCREMENTAL DECODE AND FORWARD WITH SINGLE ANTENNA NODES AND MULTIPLE RELAYS

Let us consider the cooperative SISO system with multiple relays positioned between the source and destination nodes, as shown in Fig. 5.1. We propose a comparison between the IDF relaying scheme based on relay selection, with non-cooperative schemes equipped with multiple antennas. For non-cooperative MIMO nodes, we consider the same schemes as in Chapter 4, *i.e.*, AS and SVD. Notice that the effect of reconfigurable RF amplifiers is also considered for these schemes under test. Moreover, the energy spent to transmit feedback frames, required for IDF as well as for the MIMO schemes, is also taken into account in the energy consumption model.

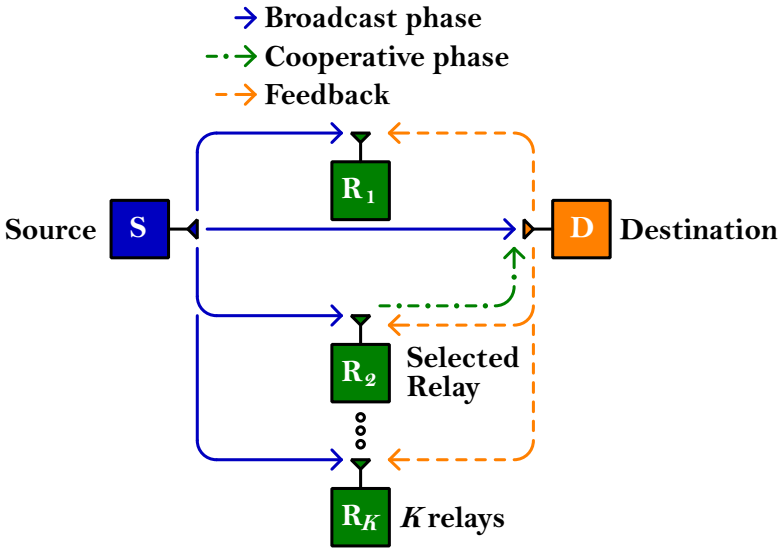

Figure 5.1: Cooperative SISO system with S, D and K relays.

5.1 Incremental Decode and Forward (IDF) Relaying

In the IDF scheme, one or two time slots can be used for the communication process. In the first time slot, the source broadcasts its message, which is received by the destination and overheard by the K relays. If the destination fails to decode the message from the source in the broadcast phase, then it replies with a NACK signal via feedback channel asking for a retransmission from the relay. Then, in the second time slot, the relay retransmits the message from the source, only if it has been successfully decoded in the broadcast phase. Finally, the destination combines the signals received from the source and relay nodes using a MRC scheme (GOLDSMITH, 2005). Moreover, in the cooperative phase, we consider an opportunistic relay selection scheme (BLETSAS et al., 2006). Notice that each relay node is able to estimate its own channel state information (CSI) with respect to the destination using the NACK message from the destination node in the cooperative phase. Thus, in possession of γ_{RD}, each relay waits for a time $t_{\mathrm{R}} \propto 1/\gamma_{\mathrm{RD}}$ before transmitting. In addition, when a retransmission occurs, we assume a carrier sense multiple access with collision avoidance (CSMA-CA) protocol, so that collision is not considered in our analysis. Then, the node with the highest SNR with respect to the destination will be the first to retransmit the source message to the destination (YABCZNSKI et al., 2021).

Since all network links are subject to failure, the overall outage probability is modelled as (PERON; BRANTE; SOUZA, 2015)

$$\mathcal{O}_{\mathrm{IDF}} = \mathcal{O}_{\mathrm{SD}}\,\mathcal{O}_{\mathrm{SR}}^{K} + \sum_{k=1}^{K} \binom{K}{k} \mathcal{O}_{\mathrm{SR}}^{K-k}\,(1-\mathcal{O}_{\mathrm{SR}})^{k}\,\mathcal{O}_{\mathrm{SRD}}(k), \tag{5.1}$$

where the point-to-point outage probabilities at the broadcast phase are lumped as

$$\mathcal{O}_{ij} = 1 - \exp\left(-\frac{2^{\xi}-1}{\bar{\gamma}_{ij}}\right). \tag{5.2}$$

Moreover, the expression for $\mathcal{O}_{\mathrm{SRD}}(k)$ in (5.1) is a function of k and represents the MRC of the message transmitted by the source in the broadcast phase with the retransmission from

the selected relay in the cooperative phase, which can be calculated as (PERON; BRANTE; SOUZA, 2015)

$$\begin{aligned}\mathcal{O}_{\mathrm{SRD}}(k) = &\sum_{l=0}^{k-1} \binom{k-1}{l} \frac{k\,(-1)^l}{\bar{\gamma}_{\mathrm{SD}}\,(l+1) - \bar{\gamma}_{\mathrm{RD}}} \\ &\times \left\{ \bar{\gamma}_{\mathrm{SD}} \left[1 - \exp\left(-\frac{2^{\xi}-1}{\bar{\gamma}_{\mathrm{RD}}} \right) \right] - \frac{\bar{\gamma}_{\mathrm{RD}}}{l+1} \left[1 - \exp\left(-\frac{2^{\xi}-1\,(l+1)}{\bar{\gamma}_{\mathrm{RD}}} \right) \right] \right\},\end{aligned} \tag{5.3}$$

in which (5.3) assumes that $\bar{\gamma}_{\mathrm{SD}}\,(l+1) - \bar{\gamma}_{\mathrm{RD}} \neq 0$.

5.1.1 Energy Efficiency

In order to evaluate the EE, we define the total energy consumption per bit of each scheme. Following (ROSAS; OBERLI, 2012), we model the energy consumption with the appropriate modifications, that is, including the reconfigurable RF amplifiers. First, let us define the average transmission time per payload bit, which is given by (ROSAS; OBERLI, 2012)

$$T_{\mathrm{b}} = \frac{1}{R_{\mathrm{s}}} \left(\frac{1}{\xi} + \frac{H+O}{P} \right), \tag{5.4}$$

where R_{s} denotes the physical layer symbol rate, H is the size of the header, P is the size of the payload and O is a measure of the total overhead bits per forward frame.

Then, consider the cooperative network scenario presented previously in Fig. 5.1, where the communication process can be carried out in two time slots. In the first time slot, the source broadcasts its message, which is forwarded to the destination and also overheard by the K relay nodes. Thus, the energy consumption of the broadcast phase is

$$\mathcal{E}_{\mathrm{broad}} = \left[P_{\mathrm{PA,S,mode}} + P_{\mathrm{TX,S}} + P_{\mathrm{LNA,D,mode}} + P_{\mathrm{RX,D}} + K\,(P_{\mathrm{LNA,R,mode}} + P_{\mathrm{RX,R}}) \right] T_{\mathrm{b}}, \tag{5.5}$$

whereas in the second time slot, only the selected relay transmits to the destination, so that the

energy consumption of the cooperative phase is calculated as

$$\mathcal{E}_{\text{coop}} = \left(P_{\text{PA,R,mode}} + P_{\text{TX,R}} + P_{\text{LNA,D,mode}} + P_{\text{RX,D}}\right) T_{\text{b}}. \tag{5.6}$$

Moreover, let us assume that feedback frames are decoded without errors. So, we consider that the feedback frame consumes additional energy in the total energy consumption and takes T_{fb} seconds longer. Thus, the energy spent due to the feedback frame is

$$\mathcal{E}_{\text{fb}} = \left[P_{\text{PA,D,9}} + P_{\text{TX,D}} + K\left(P_{\text{LNA,R,3}} + P_{\text{RX,R}}\right)\right] T_{\text{fb}}, \tag{5.7}$$

with $T_{\text{fb}} = F/(R_{\text{s}}\, P)$, where F is the number of bits that compose the feedback frame. Also, note that the feedback transmission is from destination to K relay nodes. Then, the relay with the best transmission condition is selected to operate in the cooperative phase. Moreover, since we consider a retransmission request via an error free feedback channel, we put the reconfigurable RF amplifiers in high-performance mode in order to increase the link quality, so that the PA is in mode 9 and the LNA in mode 3.

The main difference when a feedback channel is available in the communication process is that the destination responds with a ACK/NACK frame whenever it detects the successful/failed reception at the broadcast phase. In other words, the cooperative phase will be necessary only if the destination was not able to receive the source message correctly. Next, we define the EE for the IDF scheme, including the feedback energy as

$$\eta_{\text{IDF}} = \xi \cdot \frac{(1-\mathcal{O}_{\text{SD}})}{\mathcal{E}_{\text{broad}} + \mathcal{E}_{\text{fb}}} + \frac{\xi}{2} \cdot \sum_{k=1}^{K} \binom{K}{k} \frac{\mathcal{O}_{\text{SR}}^{K-k}\,(1-\mathcal{O}_{\text{SR}})^{k}}{\mathcal{E}_{\text{broad}} + \mathcal{E}_{\text{coop}} + \mathcal{E}_{\text{fb}}} \cdot \left[\mathcal{O}_{\text{SD}} - \mathcal{O}_{\text{SRD}}(k)\right], \tag{5.8}$$

where the destination receives ξ bps/Hz if the transmission at the broadcast phase is successful or receives $\xi/2$ bps/Hz if transmission at the cooperative phase is successful. Otherwise, if the source message could not be received correctly by the destination in either of the transmission phases, the message is discarded and the instantaneous EE is considered to be zero.

5.2 Benchmark Schemes

In this section, we present the energy efficiency expressions for the non-cooperative MIMO schemes, with the main modification with respect to Chapter 4 being the inclusion of the feedback channel, which is required for AS in order to select the best antenna at the transmitter, and required for SVD in order to design precoding and equalization matrices.

5.2.1 Antenna Selection (AS)

As in Section 4.2, only one antenna is active at both transmitter and receiver, which reduces the power consumption due to the reduced number of RF chains. The pair of antennas can be chosen during the transmission of pilot symbols prior to each frame, in which the best antenna at the receiver is selected based on the highest received SNR, whereas a feedback channel is required in order to inform the index of the selected antenna to the transmitter, also based on the highest instantaneous SNR. Let us remark that a small number of feedback bits is usually required for AS, in the order of $\log_2(N_{\mathrm{S}})$ (KRAUSS et al., 2019). The outage probability of AS is given in (4.6), which we reproduce here for an easier visualization

$$\mathcal{O}_{\mathrm{AS}} = \left[1 - \exp\left(-\frac{2^{\xi}-1}{\bar{\gamma}_{\mathrm{SD}}}\right)\right]^{N_{\mathrm{S}}\,N_{\mathrm{D}}}. \tag{5.9}$$

Moreover, the total power consumption including the feedback energy is

$$\begin{aligned} P_{\mathrm{AS}} = &\left(P_{\mathrm{PA,S,mode}} + P_{\mathrm{TX,S}} + P_{\mathrm{LNA,D,mode}} + P_{\mathrm{RX,D}}\right) T_{\mathrm{b}} \\ &+ \left(P_{\mathrm{PA,D,9}} + P_{\mathrm{TX,D}} + P_{\mathrm{LNA,S,3}} + P_{\mathrm{RX,S}}\right) T_{\mathrm{fb}}, \end{aligned} \tag{5.10}$$

and the EE of AS is calculated as

$$\eta_{\mathrm{AS}} = \xi \cdot \frac{(1-\mathcal{O}_{\mathrm{AS}})}{P_{\mathrm{AS}}}. \tag{5.11}$$

5.2.2 Singular Value Decomposition (SVD) Beamforming

In this scheme, all antennas are used at the transmitter and receiver nodes, which increases the robustness to channel fading, but also increases the power consumption due to the number of active RF chains. In addition, a feedback channel is also required for SVD; however, the capacity of the feedback channel must be much higher than in the case of AS. Let us remark that the complex realization of the channels are required for SVD in order to design the precoding matrix at the transmitter, including both phase and amplitude information. In the literature, it is usual to assume that the magnitude can be fed back with as low as a 1-bit quantization scheme, while b bits are used for the phase information, by employing a codebook consisting of 2^b N_{S}-dimentional elements (YOO; JINDAL; GOLDSMITH, 2007; KRAUSS et al., 2019), *i.e.*, the receiver quantizes the channel phase of each receive antenna to one of the elements in the codebook, then such codebook indexes are fed back to the transmitter. In this case, $N_{\mathrm{S}}\,(b+1)$ feedback bits are required for SVD.

Recalling (4.10), the outage probability of SVD is

$$\mathcal{O}_{\mathrm{SVD}} \geq 1 - \exp\left(-\frac{\rho}{\bar{\gamma}_{\mathrm{SD}}}\right) \sum_{m=0}^{N_{\mathrm{S}}\,N_{\mathrm{D}}-1} \frac{1}{m!} \left(\frac{\rho}{\bar{\gamma}_{\mathrm{SD}}}\right)^{m}, \tag{5.12}$$

where $\rho = n\,\left(2^{\xi/n}-1\right)$ with $n = \min\{N_{\mathrm{S}}, N_{\mathrm{D}}\}$. The total power consumption of SVD is

$$\begin{aligned} P_{\mathrm{SVD}} = {} & \left[N_{\mathrm{S}}\,\left(P_{\mathrm{PA,S,mode}} + P_{\mathrm{TX,S}}\right) + N_{\mathrm{D}}\,\left(P_{\mathrm{LNA,D,mode}} + P_{\mathrm{RX,D}}\right)\right] T_{\mathrm{b}} \\ & + \left[N_{\mathrm{D}}\,\left(P_{\mathrm{PA,D,9}} + P_{\mathrm{TX,D}}\right) + N_{\mathrm{S}}\,\left(P_{\mathrm{LNA,S,3}} + P_{\mathrm{RX,S}}\right)\right] T_{\mathrm{fb,SVD}}, \end{aligned} \tag{5.13}$$

where $T_{\mathrm{fb,SVD}} = F_{\mathrm{SVD}}/(R_{\mathrm{s}}\,P)$. Note that due to the use of all antennas in the SVD scheme, the total power consumption is higher compared to the AS scheme.

Finally, the EE of SVD is represented by

$$\eta_{\mathrm{SVD}} = \xi \cdot \frac{(1-\mathcal{O}_{\mathrm{SVD}})}{P_{\mathrm{SVD}}}. \tag{5.14}$$

5.3 Optimization Problem

We propose the EE optimization for the IDF scheme, also selecting the best operating mode for the PA and LNA circuits, as follows

$$\begin{aligned} \max_{P_{i,\text{mode}},\, F_{j,\text{mode}}} \quad & \eta_{\text{IDF}}, \\ \text{s.t.} \quad & P_{i,\text{mode}} \in \mathcal{S}_{\text{PA}}, \\ & F_{j,\text{mode}} \in \mathcal{S}_{\text{LNA}}, \\ & \mathcal{O}_{(\text{sch})} \leq \mathcal{O}^{\star}. \end{aligned} \tag{5.15}$$

It is worth mentioning that in this chapter, the SE is kept unchanged for the sake of simplicity in the comparison between the transmission schemes, in which we consider $\xi = 2$. In addition, we remind that the operating modes of the PA transmission power $P_{i,\text{mode}} \in [1, 9]$, according to Table 3.1 and the operating modes of the LNA noise factor $F_{j,\text{mode}} \in [1, 3]$, according to Table 3.2. Then, we resort to an exhaustive search to solve our optimization problem in (5.15).

In Algorithm 2, we can notice that if the transmission from the source to the destination occurred successfully in the broadcast phase, then the second time slot will not be necessary and, therefore, energy savings will be obtained. Moreover, it is important to mention that if the cooperative phase occurs, then the energy consumption spent by the relay for retransmitting the source message to the destination will be computed, even if this transmission fails in the second time slot.

Algorithm 2 EE maximization for the IDF scheme.

Input: d_{ij}, $\mathcal{O}^{\star}$

$index \leftarrow 1$; $\eta_{\mathrm{IDF},index-1} \leftarrow 0$
for $P_{\mathrm{S,mode}} \in \mathcal{S}_{\mathrm{PA}}$ **do**
  for $F_{\mathrm{D,mode}} \in \mathcal{S}_{\mathrm{LNA}}$ **do**
    ; compute $[P_{\mathrm{S,mode}} - \mathrm{PAPR}(\xi)] \rightarrow$ in [dB]
    ; compute $F_{\mathrm{D,mode}}$ using (3.1)
    ; compute $P_{\mathrm{PA,S,mode}}$ and $P_{\mathrm{LNA,D,mode}}$
    ; compute κ_{SD} and $\bar{\gamma}_{\mathrm{SD}}$ using (3.3) and (3.5)
    ; compute $\mathcal{O}_{\mathrm{SD}}$ using (5.2)
    for $F_{\mathrm{R,mode}} \in \mathcal{S}_{\mathrm{LNA}}$ **do**
      ; compute $F_{\mathrm{R,mode}}$ using (3.1)
      ; compute $P_{\mathrm{LNA,R,mode}}$
      ; compute $\mathcal{E}_{\mathrm{broad}}$ using (5.5)
      ; compute $\mathcal{E}_{\mathrm{fb}}$ using (5.7)
      ; compute κ_{SR} and $\bar{\gamma}_{\mathrm{SR}}$ using (3.3) and (3.5)
      ; compute $\mathcal{O}_{\mathrm{SR}}$ using (5.2)
      if $\mathcal{O}_{\mathrm{SD}} > \mathcal{O}^{\star}$ **then**
        for $P_{\mathrm{R,mode}} \in \mathcal{S}_{\mathrm{PA}}$ **do**
          for $F_{\mathrm{D,mode}} \in \mathcal{S}_{\mathrm{LNA}}$ **do**
            ; compute $[P_{\mathrm{R,mode}} - \mathrm{PAPR}(\xi)] \rightarrow$ in [dB]
            ; compute $F_{\mathrm{D,mode}}$ using (3.1)
            ; compute $P_{\mathrm{PA,R,mode}}$ and $P_{\mathrm{LNA,D,mode}}$
            ; compute $\mathcal{E}_{\mathrm{coop}}$ using (5.6)
            ; compute κ_{RD} and $\bar{\gamma}_{\mathrm{RD}}$ using (3.3) and (3.5)
            ; compute $\mathcal{O}_{\mathrm{RD}}$ using (5.2)
            ; compute $\mathcal{O}_{\mathrm{IDF}}$ using (5.1)
            if $\mathcal{O}_{\mathrm{IDF}} > \mathcal{O}^{\star}$ **then**
              $\eta_{\mathrm{IDF},index} \leftarrow 0$
            else
              ; compute $\eta_{\mathrm{IDF},index}$ using (5.8)
              if $\eta_{\mathrm{IDF},index} < \eta_{\mathrm{IDF},index-1}$ **then**
                $\eta_{\mathrm{IDF},index} \leftarrow \eta_{\mathrm{IDF},index-1}$
              end if
            end if
          end for
        end for
      else
        ; compute $\mathcal{E}_{\mathrm{coop}} \leftarrow 0$
        ; compute $\eta_{\mathrm{IDF},index}$ using (5.8)
        if $\eta_{\mathrm{IDF},index} < \eta_{\mathrm{IDF},index-1}$ **then**
          $\eta_{\mathrm{IDF},index} \leftarrow \eta_{\mathrm{IDF},index-1}$
        end if
      end if
    end for
  end for
end for

Output: $\eta_{\mathrm{IDF},index}$

5.4 Numerical Results

In this section, we present some numerical results in order to assess the EE. Let us remark that our goal is to combine cooperative communication through the IDF scheme with the reconfigurability of the PA and LNA circuits. The simulation parameters are defined in Table 5.1. According to (KRAUSS et al., 2019), as low as $b = 1$ quantization bits can be used depending on the system requirements, which implies in $2^b\, N_{\mathrm{S}}$ feedback bits for SVD, compared to $\log_2(N_{\mathrm{S}})$ bits for AS. In order to provide some numerical examples, we have considered that SVD requires a feedback frame that is twice that of AS and IDF. Moreover, note that $N_{\mathrm{S}}\, N_{\mathrm{D}} = K - 1$ is necessary for a fair comparison in terms of diversity order. Therefore, when setting for the MIMO schemes ($N_{\mathrm{S}} = 1$ and $N_{\mathrm{D}} = 2$) or ($N_{\mathrm{S}} = 2$ and $N_{\mathrm{D}} = 1$), we consider $K = 1$ for IDF and, when applying ($N_{\mathrm{S}} = N_{\mathrm{D}} = 2$) for the MIMO schemes, then $K = 3$ must be set to IDF.

Table 5.1: System parameters for cooperative communication.

Parameter	Description	Value
R_{s}	symbol rate	10 kBd †
P	forward payload frame length	98 bytes †
H	forward header frame length	2 bytes †
O	forward overhead frame length	5 bytes †
F	feedback frame length for IDF and AS	11 bytes †
F_{SVD}	feedback frame length for SVD	22 bytes
ξ	spectral efficiency	2 bps/Hz
B	bandwidth	180 kHz §
L	link margin	20 dB
f_{c}	carrier frequency	2.4 GHz
A	total antenna gain	5 dBi ‡
α	path loss exponent	2.5 ‡
$\mathcal{O}^{\star}$	target outage probability	10^{-3} ‡
N_0	noise power spectral density	-174 dBm/Hz ‡
$P_{\mathrm{TX},i}$	non-reconf. TX power consumption	98 mW ‡
$P_{\mathrm{RX},j}$	non-reconf. RX power consumption	94.4 mW ‡

§Source: (3GPP TR 36.888, 2013),
†Source: (ROSAS; OBERLI, 2012),
‡Source: (NAEEM; PATWARY; ABDEL-MAGUID, 2017).

Fig. 5.2 compares the EE of IDF with the non-cooperative MIMO schemes, where the number of relays is $K = 1$, with $N_{\mathrm{S}} = 1$ and $N_{\mathrm{D}} = 2$ for the MIMO schemes in Fig. 5.2a, and $N_{\mathrm{S}} = 2$ and $N_{\mathrm{D}} = 1$ in Fig. 5.2b. Fig. 5.2a depicts that the AS performs better in terms of EE

than the other schemes, which is justified since this scheme has the lowest power consumption at the circuit level. On the other hand, the IDF scheme is the method that reaches the longest transmission distance, outperforming SVD both in terms of EE and transmission range. For the communication scenario proposed in Fig. 5.2b, we can observe a slight improvement in EE for the SVD and an increase in the transmission range due to the set of 2×1 antennas.

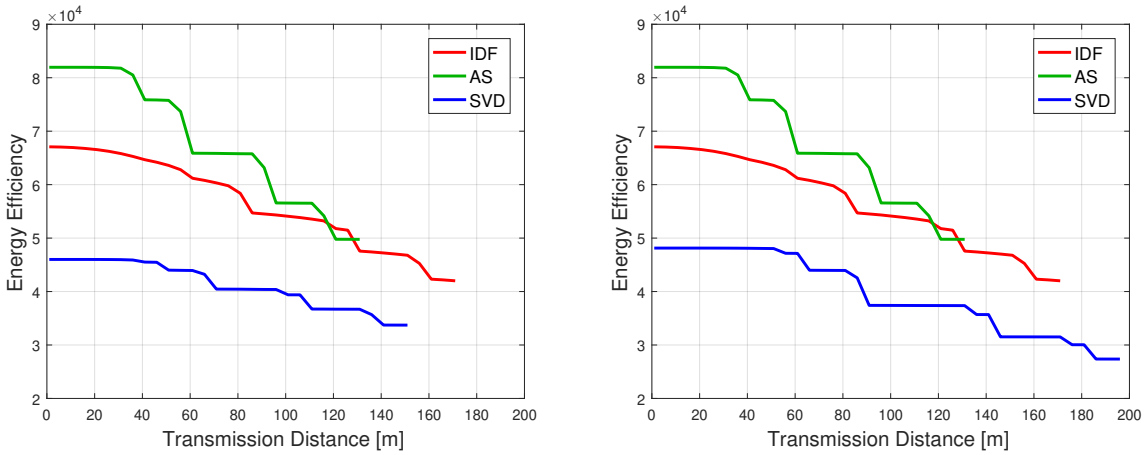

(a) MIMO (1×2) and $K = 1$.

(b) MIMO (2×1) and $K = 1$.

Figure 5.2: EE comparison between IDF, AS and SVD schemes, with the relay positioned at $d_{\mathrm{SR}} = 0.5\, d_{\mathrm{SD}}$.

Next, Fig. 5.3 depicts a scenario with MIMO (2×2) and $K = 3$. Similarly to the previous analysis, the AS scheme achieves the highest EE among the considered schemes. Furthermore, we note that there is a trade-off between IDF and SVD, in which IDF performs better over short distances, while SVD reaches longer transmission distances, for the same target outage probability. Through this analysis, we can see that the schemes under test show different EE results, which depend mainly on the diversity order adopted in each communication system.

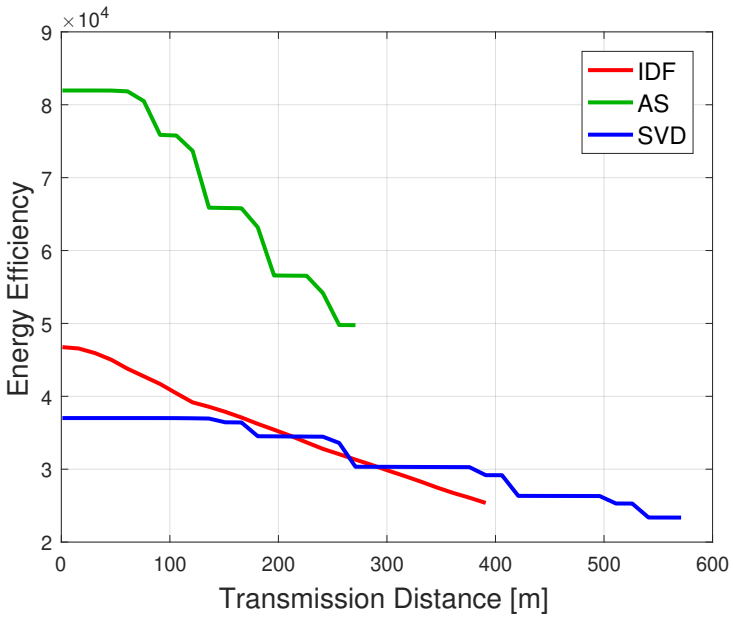

Figure 5.3: EE of IDF, AS and SVD, with MIMO (2×2) and $K = 3$, with the relays positioned at $d_{\mathrm{SR}} = 0.5\, d_{\mathrm{SD}}$.

In Figs. 5.4-5.6, we show how the reconfigurable PA and LNA circuits operate for the cooperative relaying scheme, with the one relay positioned at different distances between the source and the destination, that is, $d_{\mathrm{SR}} = 0.2\, d_{\mathrm{SD}}$, $d_{\mathrm{SR}} = 0.5\, d_{\mathrm{SD}}$ and $d_{\mathrm{SR}} = 0.8\, d_{\mathrm{SD}}$, respectively. Moreover, note that the figure on the left represents the S-D link, the one in the middle is the S-R link, while the one in the right is the R-D link. First, analyzing the broadcast phase, it is worth noting that at a specific distance the PA transmits the same amount of power to the destination and relay nodes, then the PA switches to a higher transmission power mode only when the distance increases. Besides that, only during transmission between the S-R nodes, we notice that the LNA presents different results in switching operating modes, which is justified with the relay located at different distances.

Furthermore, analyzing the retransmission phase, we observe that an efficient adaptation protocol is required. This can be achieved during the handshake phase in order to obtain the channel estimates and reconfigure the transmitter and receiver circuits, as needed. Moreover, since the relay operates only if necessary, results show that the relay is responsible for most of the reconfigurability, then the LNA and PA circuits tend to switch their operating modes more frequently. As we can see in Fig. 5.4, the relay being closer to the source presents a more significant interaction, which in this case means that the relay cooperates more in the

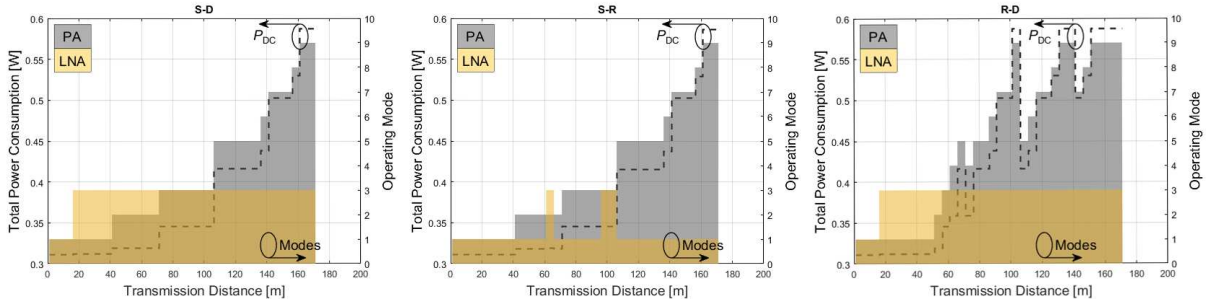

Figure 5.4: Total power consumption in each point-to-point transmission and best operating mode for the PA and LNA circuits, with the relay positioned at $d_{\mathrm{SR}} = 0.2\, d_{\mathrm{SD}}$.

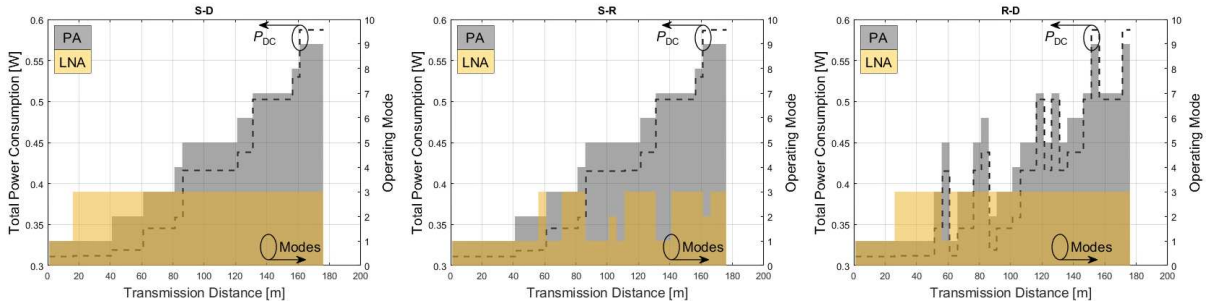

Figure 5.5: Total power consumption in each point-to-point transmission and best operating mode for the PA and LNA circuits, with the relay positioned at $d_{\mathrm{SR}} = 0.5\, d_{\mathrm{SD}}$.

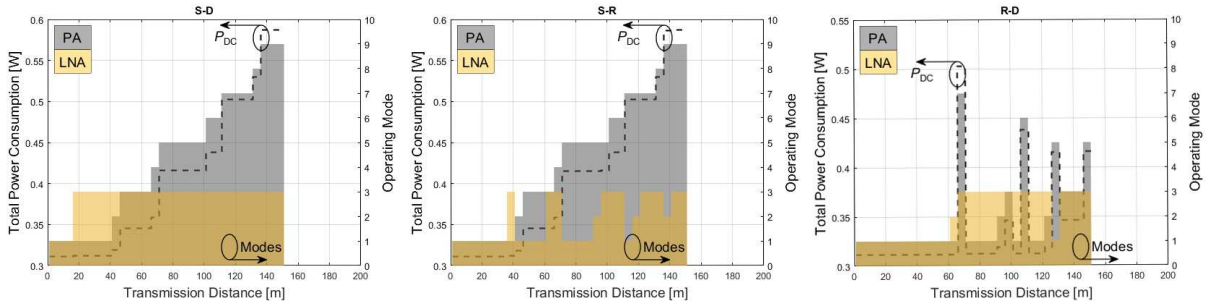

Figure 5.6: Total power consumption in each point-to-point transmission and best operating mode for the PA and LNA circuits, with the relay positioned at $d_{\mathrm{SR}} = 0.8\, d_{\mathrm{SD}}$.

retransmission. Whereas Fig. 5.6 shows the relay close to the destination, that is, we can observe low activity in the PA and LNA operation modes. Finally, another important observation is that there is an optimal position for the relay node, in our examples a greater communication distance together with the EE is maximized with the relay positioned in the middle between the source and destination nodes, as shown in Fig. 5.5.

5.4.1 Considerations About Optimizing the Number of Relays

Fig. 5.7a illustrates the optimum number of relays, considering the range $1 \leq K \leq 10$, with the joint optimization of the PA and LNA operating modes that maximizes the EE. From the figure, we can see that the optimum number of relays increases according to the communication distance. Also, notice that by increasing the number of relays, longer distances are attainable. Moreover, it is worth mentioning that the number of relays applied in this example is small, which makes it feasible in practice. Furthermore, Fig. 5.7b presents the EE results by jointly selecting the best operating modes of the PA and LNA circuits with the optimum number of relays. Notice that the number of relays has contributed for achieving longer communication distances. When comparing this result with Fig. 5.2, we can see that for short distances there has been no increase in the EE, which is justified by the fact that the EE is maximized with fewer relays. More interestingly, it is worth mentioning that in the broadcast phase all relays hear to the source and, therefore, the greater the number of cooperative relays, the greater the power consumption at the circuit level, which impacts on the EE.

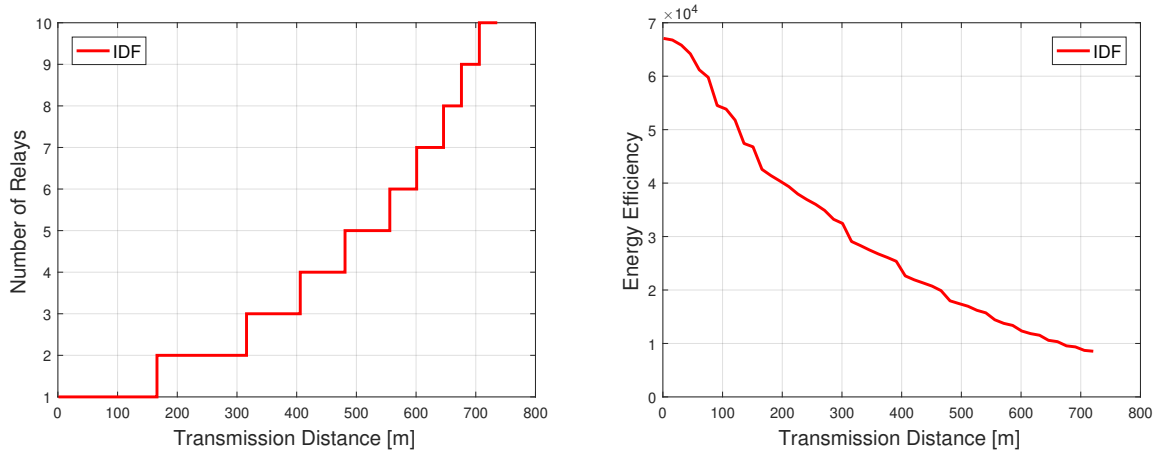

(a) (b)

Figure 5.7: (a) Optimum number of relays for the IDF scheme; (b) EE of IDF with the joint optimization of the PA and LNA operating modes and the number of relays, with the relay positioned at $d_{\mathrm{SR}} = 0.5\, d_{\mathrm{SD}}$.

5.5 Summary of the Chapter

In this chapter, the EE analysis is presented for cooperative communication. In this network scenario, we assume nodes equipped with single antenna and our system is modeled taking into account also the reconfigurability of RF amplifiers. Our goal was to compare cooperative transmissions, using the IDF scheme, aided by a feedback channel to perform relay selection, with non-cooperative schemes with multiple antennas.

Through the results, we found that the AS outperforms the others schemes in terms of EE. For the scenario MIMO (2×1) and $K = 1$, IDF outperforms the SVD scheme. In addition, by increasing the diversity order of the schemes to MIMO (2×2) and $K = 3$, we note that the AS scheme still achieves the highest EE among the considered schemes. On the other hand, a trade-off between EE and transmission distance is noted between the IDF and SVD schemes. In this case, IDF presents a higher EE over short distances, whereas the SVD allows communicating at longer transmission distances.

When evaluating the EE according to the position of the relay node, it was found through our simulations that the EE is maximized with the relay positioned in the middle between the source and destination nodes. Moreover, the results pointed out that most of the reconfigurability ends up being at the relay, since it only acts if necessary in the considered IDF protocol, whereas the switching of the PA and LNA operating modes tends to be more stable at the source and destination nodes.

Furthermore, we show that the EE is impacted by the number of relays. Therefore, an optimization of the number of relays is performed in order to maximize the EE. Through this approach, we found that increasing the number of relays also contributes for reaching longer transmission distances, which can be interesting for IoT applications. It is worth mentioning that we use a small number of relay nodes, however, our optimization problem can be easily extended to a massive network deployment. Finally, we conclude that our approach contributes significantly towards improving the EE.

CHAPTER 6

CONCLUSIONS

6.1 Final Comments

Modern IoT networks have an increasing concern towards higher energy efficiency, since wireless nodes are typically battery-powered. In this thesis, we analyzed the energy efficiency of reconfigurable circuit designs, showing that RF transceivers based on multimode operation can significantly improve the energy efficiency in wireless communication systems. In our framework, we considered state-of-the-art reconfigurable PA and LNA circuits, which are the blocks responsible for amplifying the RF signal and, thus, are typically power-hungry. Unlike most works available in the literature, our analysis carefully included real data from circuits that were previously designed and tested by simulations and measurements. We modeled the real multimode characteristic of these circuits as look-up tables, which are then handled by our optimization approach. By doing so, any other practical PA or LNA design can be integrated into our methodology. The energy efficiency was analyzed in two network scenarios, one considering non-cooperative MIMO communication and other considering cooperative SISO communication. Therefore, we carried out a joint selection of the best operating modes for the PA and LNA circuits in these communication scenarios, in order to maximize the energy efficiency. Our energy optimization approach has proven to be important for energy savings and can be used for future IoT deployments.

For the first scenario, our results show that by reconfiguring the PA operating modes at the transmitter jointly with the LNA operating modes at the receiver, an improvement in energy efficiency is achieved for short-range communications when compared to non-reconfigurable circuit designs. Numerically, the results show an EE improvement of more than 40% at distances up to 67 meters. Further, we also considered that the PA operates at different backed-off

power levels under different spectral efficiency values. Thus, we show that combining spectral efficiency with reconfigurable circuits, an even more significant gain in energy efficiency can be achieved for the same scenario under test. In addition, our results also pointed out that AS is in general more energy efficient than the other schemes in several communication scenarios, whereas SVD achieves longer distances of communication. We also show that the number of antennas for MIMO schemes contribute differently to energy efficiency. SVD presents an optimal number of antennas, since the energy efficiency decreases due to the increase of RF chains. On the other hand, the energy efficiency of the AS always increases with the number of antennas, although the increase saturates at a certain point. Finally, we conclude that reconfigurable RF transceivers are an interesting solution to reduce the energy required to an end-to-end communication, since the LNA allows to improve the SNR by adjusting its noise figure and, therefore, a lower level of transmission power at the PA output is required.

For the second scenario, we compare the performance of IDF relaying, performing relay selection, with non-cooperative MIMO schemes. In addition, we model the total energy consumption, including both the forward and feedback transmission power and the power consumption of RF circuits. Since in short-range distances the energy efficiency is mainly impacted by the power consumed by the RF circuits, then a better energy efficiency is achieved by schemes that employ antenna selection techniques at the transmitter and receiver, as it reduces power consumption. On the other hand, IDF relaying helps to achieve slightly longer transmission distances compared to antenna selection schemes. In addition, the IDF is more energy-efficient in short transmissions than SVD beamforming, while longer transmissions are achieved by the SVD, as it exploits all antennas. We also found that both the position of the relay between the source and the destination, as well as the number of relays, impact on energy efficiency. That is, the energy efficiency is maximized with the relay positioned halfway between the source and destination nodes. Moreover, results show that the most of reconfigurability of the PA and LNA circuits occurs at the relay, since it acts only if necessary. Whereas at source and destination, the reconfigurability tends to be more stable. Finally, increasing the number of relays contributes to achieving longer communication distances, at the cost of energy efficiency.

6.2 Future Works

Through the results obtained in this research, some perspectives for future works are presented as follows. Regarding the RF transceiver circuits, new reconfigurable PA and LNA architectures could be used to optimize the energy efficiency. In addition, as only the RF amplification stage circuits were tested in this research, then another possibility to improve the energy efficiency could also take into account other building blocks, such as the frequency synthesizer, since it also consumes a lot of energy in RF transceivers (SUN et al., 2021). Since the power consumption of the frequency synthesizer is directly linked to the phase noise (GAO et al., 2009), then modelling the SNR impact when deteriorating the phase noise, aiming at a lower power consumption, could be exploited in order to assess the impact on energy efficiency.

In addition, it is worth remembering that the reconfigurable RF amplifiers chosen for this work were designed for narrowband applications. Therefore, in order to meet different communication standards, the energy efficiency could also be assessed with wideband RF transceivers (LIM et al., 2018; ZHU; ZHANG; WANG, 2019). Let us remark that we evaluated the communication channel through the SNR and we resorted to an exhaustive search to solve our optimization problem. However, another possible extension could consider other metrics and test different approaches such as artificial intelligence and machine learning to assist in switching the operating modes of the RF transceiver circuits. An example of this approach can be found in the work developed by (BANERJEE et al., 2017).

Regarding the communication scenario, different techniques could be exploited to obtain more reliable communication and, therefore, reduce the overall system energy consumption to improve efficiency. In this research we approached MIMO and cooperative communications separately. However, a suggestion would be to combine them and assess the energy efficiency with reconfigurable RF transceivers. In addition, only Rayleigh fading was considered, where there is non-line-of-sight between the transmitter and the receiver. However, in massive networks there may be situations with line-of-sight between nodes, where in this case the Nakagami-m distribution (SIMON; ALOUINI, 2008) could be employed.

Furthermore, as an immediate extension of the research work presented in this thesis, we are considering investigating the performance of a cooperative protocol with a higher code rate and diversity order, based on network coding. The concept of network coding (LI; YEUNG; CAI, 2003; KOETTER; MEDARD, 2003) applied into cooperative communications can significantly help to increase the efficient use of network resources (NOSRATINIA; HUNTER; HEDAYAT, 2004; LANEMAN, 2004). For instance, in a network coded cooperation, users are able to combine their own information and that of their partners, rather than keeping information from different users separate in different orthogonal channels. The dynamic network coding (DNC) scheme proposed by (XIAO; SKOGLUND, 2009) performs linear combinations of all available information at the relay user. That is, after broadcasting their own information, each user transmits in the cooperative phase $U - 1$ non-binary linear combinations of information over a large enough Galois Field GF(q), which improves the diversity order. In (REBELATTO et al., 2012), the DNC scheme was extended allowing each user to broadcast several (as opposed to just one) messages in the broadcast phase, as well as to transmit several non-binary linear combinations in the cooperative phase. The Generalized DNC (GDNC) scheme, besides improving error performance, was shown to be capable of simultaneously achieving both code rate and diversity order higher than the other schemes. Moreover, a feedback-assisted version of the GDNC scheme, called FA-GDNC, was proposed in (REBELATTO et al., 2011), aiming to increase the average code rate without degrading the system error performance. Motivated by the GDNC gains and the reconfigurable RF transceivers, we intend to combine them in order to evaluate the energy efficiency.

6.3 Published Papers

Listed below are the papers published so far, related to the theme of this research.

2 Journals

- JUNIOR, E. N.; THEIS, G.; **SANTOS, E. L.**; MARIANO, A. A.; BRANTE, G.; SOUZA, R. D.; TARIS, T.. Energy Efficiency Analysis of MIMO Wideband RF Front-End Re-

ceivers. **SENSORS**, v. 20, p. 7070, 2020. DOI: 10.3390/s20247070.

- **SANTOS, E. L.**; MARIANO, A. A.; BRANTE, G.; LEITE, B.; SOUZA, R. D.; TARIS, T.. Energy Efficiency in Multiple Antenna Machine-Type Communications With Reconfigurable RF Transceivers. **IEEE Access**, v. 7, p. 113031-113042, 2019. DOI: 10.1109/ACCESS.2019.2934641.

2 National Symposiums

- **SANTOS, E. L.**; MARIANO, A. A.; BRANTE, G.; SOUZA, R. D.. Energy Analysis in Cooperative Machine-Type Communications with Reconfigurable RF Transceivers. **XXXVIII Simpósio Brasileiro de Telecomunicações e Processamento de Sinais (SBrT)**, 2020, Florianópolis. DOI: 10.14209/SBRT.2020.1570648622.

- TARUI, B. Y.; SANTOS, F. G.; **SANTOS, E. L.**; LEITE, B.; MARIANO, A. A.. Multimode 2.4 GHz CMOS Power Amplifier with Gain and Power Control. **XXXIII Simpósio Sul de Microeletrônica (SIM)**, 2018, Curitiba.

1 International Symposium

- TARUI, B.; SANTOS, F.; **SANTOS, E. L.**; LEITE, B.; MARIANO, A. A.. Design of an RF Six-Mode CMOS Power Amplifier for Efficiency Improvement at Power Backoff. **31st Symposium on Integrated Circuits and Systems Design (SBCCI)**, 2018, Bento Gonçalves. DOI: 10.1109/SBCCI.2018.8533222.

BIBLIOGRAPHY

3GPP TR 21.914. *Release 14 Description*. [S.l.], May 2018. Available in: <portal.3gpp.org/desktopmodules/Specifications/SpecificationDetails.aspx?specificationId=3179>.

3GPP TR 36.888. *Study on provision of low-cost Machine-Type Communications (MTC) User Equipments (UEs) based on LTE.* [S.l.], June 2013. Available in: <portal.3gpp.org/desktopmodules/Specifications/SpecificationDetails.aspx?specificationId=2578>.

BANERJEE, A.; DING, L.; HEZAR, R. A high efficiency multi-mode outphasing RF power amplifier with 31.6 dBm peak output power in 45nm cmos. **IEEE Transactions on Circuits and Systems I: Regular Papers**, v. 67, n. 3, p. 815–828, 2020.

BANERJEE, D. et al. Self-learning rf receiver systems: Process aware real-time adaptation to channel conditions for low power operation. **IEEE Transactions on Circuits and Systems I: Regular Papers**, v. 64, n. 1, p. 195–207, 2017.

BEHRTCH. **2021 IoT Predictions: 10 Experts Weigh-In**. [S.l.], January 2021. Available in: <www.behrtech.com/blog/2021-iot-predictions-10-experts-weigh-in/>.

BISHT, R.; QURESHI, S. Design of low-power reconfigurable low-noise amplifier with enhanced linearity. In: **TENCON 2019 - 2019 IEEE Region 10 Conference (TENCON)**. [S.l.: s.n.], 2019. p. 1216–1219.

BLETSAS, A. et al. A simple cooperative diversity method based on network path selection. **IEEE Journal on Selected Areas in Communications**, v. 24, n. 3, p. 659–672, 2006.

BOUGARD, B. et al. Smartmimo: An energy-aware adaptive mimo-ofdm radio link control for next-generation wireless local area networks. **EURASIP Journal on Wireless Communications and Networking**, v. 2007, 07 2007.

BRANTE, G.; KAKITANI, M. T.; SOUZA, R. D. Energy efficiency analysis of some cooperative and non-cooperative transmission schemes in wireless sensor networks. **IEEE Trans. Commun.**, v. 59, n. 10, p. 2671–2677, Oct. 2011. ISSN 0090-6778.

BRANTE, G. et al. Outage probability and energy efficiency of cooperative MIMO with antenna selection. **IEEE Trans. Wireless Commun.**, v. 12, n. 11, p. 5896–5907, Nov. 2013.

CHANG, S.; SHIN, H. 2.4-GHz CMOS bluetooth RF receiver with improved IM2 distortion tolerance. **IEEE Transactions on Microwave Theory and Techniques**, v. 68, n. 11, p. 4589–4598, 2020.

CHEN, J. et al. Intelligent massive MIMO antenna selection using monte carlo tree search. **IEEE Transactions on Signal Processing**, v. 67, n. 20, p. 5380–5390, 2019.

CICCIA, S.; GIORDANENGO, G.; VECCHI, G. Energy efficiency in IoT networks: Integration of reconfigurable antennas in ultra low-power radio platforms based on system-on-chip. **IEEE Internet of Things Journal**, v. 6, n. 4, p. 6800–6810, 2019.

CISCO. **Cisco Annual Internet Report (2018?2023)**. [S.l.], March 2020. Available in: <www.cisco.com/c/en/us/solutions/collateral/executive-perspectives/annual-internet-report-/white-paper-c11-741490.html?dtid=osscdc000283>.

CLERCKX, B. et al. Fundamentals of wireless information and power transfer: From RF energy harvester models to signal and system designs. **IEEE Journal on Selected Areas in Communications**, v. 37, n. 1, p. 4–33, 2019.

COVER, T.; GAMAL, A. E. Capacity theorems for the relay channel. **IEEE Transactions on Information Theory**, v. 25, n. 5, p. 572–584, 1979.

CRIPPS, S. C. **RF Power Amplifiers for Wireless Communications**. 2nd. ed. [S.l.]: Artec House, 2006.

CUI, S.; GOLDSMITH, A.; BAHAI, A. Energy-efficiency of MIMO and cooperative MIMO techniques in sensor networks. **IEEE J. Sel. Areas Commun.**, v. 22, n. 6, p. 1089–1098, Aug. 2004. ISSN 0733-8716.

____. Energy-constrained modulation optimization. **IEEE Trans. Wireless Commun.**, v. 4, n. 5, p. 2349–2360, Sep. 2005. ISSN 1536-1276.

DU, R.; SHOKRI-GHADIKOLAEI, H.; FISCHIONE, C. Wirelessly-powered sensor networks: Power allocation for channel estimation and energy beamforming. **IEEE Transactions on Wireless Communications**, v. 19, n. 5, p. 2987–3002, 2020.

ESKANDARI, M. et al. Antenna selection and power allocation for energy efficient MIMO systems. **Journal of Communications and Networks**, v. 20, n. 6, p. 546–553, 2018.

FRIIS, H. T. Noise figures of radio receivers. **Proceedings of the IRE**, v. 32, n. 7, p. 419–422, July 1944. ISSN 0096-8390.

GAO, X. et al. Jitter analysis and a benchmarking figure-of-merit for phase-locked loops. **IEEE Transactions on Circuits and Systems II: Express Briefs**, v. 56, n. 2, p. 117–121, 2009.

GE, X.; ZHANG, W. Energy efficiency of 5g wireless communications. **5G Green Mobile Communication Networks**, p. 29–101, 2019.

GHASRI, M. A. G. et al. Novel relay selection algorithms for machine-to-machine communications with static RF interfaces setting. **IEEE Access**, v. 8, p. 189989–190008, 2020.

GILASGAR, M.; BARLABÉ, A.; PRADELL, L. A 2.4 GHz CMOS class-F power amplifier with reconfigurable load-impedance matching. **IEEE Transactions on Circuits and Systems I: Regular Papers**, v. 66, n. 1, p. 31–42, 2019.

GKOUTIS, P.; KOLIOS, V.; KALIVAS, G. A reconfigurable 2.4GHz power amplifier for polar transmitters in 28nm FD-SOI CMOS technology. In: **2019 27th Telecommunications Forum (TELFOR)**. [S.l.: s.n.], 2019. p. 1–4.

GOLDSMITH, A. **Wireless Communications**. 1st. ed. [S.l.]: Cambridge University Press, 2005.

GUO, S.; ZHOU, X.; ZHOU, X. Energy-efficient resource allocation in swipt cooperative wireless networks. **IEEE Systems Journal**, v. 14, n. 3, p. 4131–4142, 2020.

GUSTAVSSON, U. et al. Implementation challenges and opportunities in beyond-5G and 6G communication. **IEEE Journal of Microwaves**, v. 1, n. 1, p. 86–100, 2021.

HANNULA, J. et al. Performance analysis of frequency-reconfigurable antenna cluster with integrated radio transceivers. **IEEE Antennas and Wireless Propagation Letters**, v. 17, n. 5, p. 756–759, 2018.

HAYATI, M.; SHEIKHI, A.; GREBENNIKOV, A. Class-F power amplifier with high power added efficiency using bowtie-shaped harmonic control circuit. **IEEE Microwave and Wireless Components Letters**, v. 25, n. 2, p. 133–135, 2015.

i-SCOOP. **NB-IoT explained: a complete guide to Narrowband-IoT**. 2019. Acessado em: 08-02-2021. Available in: <www.i-scoop.eu/internet-of-things-guide/lpwan/nb-iot-narrowband-iot/>.

IoT-ANALYTICS. **State of the IoT 2020: 12 billion IoT connections, surpassing non-IoT for the first time**. [S.l.], November 2020. Available in: <www.iot-analytics.com/state-of-the-iot-2020-12-billion-iot-connections-surpassing-non-iot-for-the-first-time/>.

JIN, G. et al. Antenna selection in TDD massive MIMO systems. **Mobile Networks and Applications**, 06 2019.

KAZEMI, M.; MOHAMMADI, A.; DUMAN, T. M. Analysis of DF relay selection in massive MIMO systems with hardware impairments. **IEEE Transactions on Vehicular Technology**, v. 69, n. 6, p. 6141–6152, 2020.

KHALILI, A. et al. Antenna selection strategy for energy efficiency maximization in uplink OFDMA networks: A multi-objective approach. **IEEE Transactions on Wireless Communications**, v. 19, n. 1, p. 595–609, 2020.

KOETTER, R.; MEDARD, M. An algebraic approach to network coding. **IEEE/ACM Transactions on Networking**, v. 11, n. 5, p. 782–795, 2003.

KRAUSS, R. et al. Area energy efficiency of antenna selection in limited feedback device-to-device networks. **IEEE Wireless Communications Letters**, v. 8, n. 3, p. 949–952, 2019.

KUMAR, A. R. A.; DUTTA, A.; SAHOO, B. D. A low-power reconfigurable narrow-band/wideband LNA for cognitive radio-wireless sensor network. **IEEE Transactions on Very Large Scale Integration (VLSI) Systems**, v. 28, n. 1, p. 212–223, 2020.

LANEMAN, J. N. Network coding gain of cooperative diversity. In: **IEEE MILCOM 2004. Military Communications Conference, 2004.** [S.l.: s.n.], 2004. v. 1, p. 106–112 Vol. 1.

LANEMAN, J. N.; TSE, D. N. C.; WORNELL, G. W. Cooperative diversity in wireless networks: Efficient protocols and outage behavior. **IEEE Transactions on Information Theory**, v. 50, n. 12, p. 3062–3080, 2004.

LI, S. . R.; YEUNG, R. W.; CAI, N. Linear network coding. **IEEE Transactions on Information Theory**, v. 49, n. 2, p. 371–381, 2003.

LIANG, X. et al. Cooperative communications with relay selection for wireless networks: design issues and applications. **Wireless Communications and Mobile Computing**, v. 13, n. 8, p. 745–759, 2013. Available in: <www.onlinelibrary.wiley.com/doi/abs/10.1002/wcm.1138>.

LIM, K. et al. A 65-nm CMOS 2×2 MIMO multi-band LTE RF transceiver for small cell base stations. **IEEE Journal of Solid-State Circuits**, v. 53, n. 7, p. 1960–1976, 2018.

LIU, Z.; DU, W.; SUN, D. Energy and spectral efficiency tradeoff for massive MIMO systems with transmit antenna selection. **IEEE Transactions on Vehicular Technology**, v. 66, n. 5, p. 4453–4457, 2017.

LU, Y.; ZHENG, X. 6G: A survey on technologies, scenarios, challenges, and the related issues. **Journal of Industrial Information Integration**, v. 19, p. 100158, 2020. ISSN 2452-414X. Available in: <www.sciencedirect.com/science/article/pii/S2452414X20300339>.

MARINELLO, J. C. et al. Antenna selection for improving energy efficiency in XL-MIMO systems. **IEEE Transactions on Vehicular Technology**, v. 69, n. 11, p. 13305–13318, 2020.

MAXIM INTEGRATED. **2.4GHz to 2.5GHz 802.11g/b RF Transceiver, PA, and Rx/Tx/Antenna Diversity Switch**. [S.l.], April 2011. Available in: <www.maximintegrated-.com/en/products/comms/wireless-rf/MAX2830.html>.

MENDONÇA, M. O. K. et al. Antenna selection in massive MIMO based on greedy algorithms. **IEEE Transactions on Wireless Communications**, v. 19, n. 3, p. 1868–1881, 2020.

MEULEN, E. C. V. D. Three-terminal communication channels. **Advances in Applied Probability**, Cambridge University Press, v. 3, n. 1, p. 120?154, 1971.

MODESTO, A. A. et al. Linearity characterization of a multimode CMOS power amplifier for IEEE 802.11n, IEEE 802.11ax and LTE signals. In: **Simpósio Sul de Microeletrônica (SIM)**. [S.l.: s.n.], 2018.

MODESTO, A. A. et al. A CMOS power amplifier with reconfigurable power cells and matching network for 2.4 GHz wireless communications. **AEU - International Journal of Electronics and Communications**, v. 111, p. 152919, 09 2019.

MOLISCH, A. F.; WIN, M. Z. MIMO systems with antenna selection. **IEEE Microwave Magazine**, v. 5, n. 1, p. 46–56, 2004.

NAEEM, M. K.; PATWARY, M.; ABDEL-MAGUID, M. Universal and dynamic clustering scheme for energy constrained cooperative wireless sensor networks. **IEEE Access**, v. 5, p. 12318–12337, 2017. ISSN 2169-3536.

NOSRATINIA, A.; HUNTER, T. E.; HEDAYAT, A. Cooperative communication in wireless networks. **IEEE Communications Magazine**, v. 42, n. 10, p. 74–80, 2004.

NXP. **Practical Considerations for Low Noise Amplifier Design**. [S.l.], May 2013. Available in: <www.nxp.com/docs/en/white-paper/RFLNAWP.pdf>.

OSSEIRAN, A. et al. IoT and machine type communications. **IEEE Communications Standards Magazine**, v. 4, n. 2, p. 40–40, 2020.

OUYANG, C. et al. Receive antenna selection under discrete inputs: Approximation and applications. **IEEE Transactions on Communications**, v. 68, n. 4, p. 2634–2647, 2020.

PATHAK, D. et al. An ultra low power 2.4GHz sub-threshold LNA with tunable input matching for wireless sensor network applications. In: **2020 IEEE International Conference on Semiconductor Electronics (ICSE)**. [S.l.: s.n.], 2020. p. 73–76.

PERON, G. S.; BRANTE, G.; SOUZA, R. D. Energy-efficient distributed power allocation with multiple relays and antenna selection. **IEEE Trans. Commun.**, v. 63, n. 12, p. 4797–4808, Dec. 2015.

REBELATTO, J. L. et al. Adaptive distributed network-channel coding for cooperative multiple access channel. In: **2011 IEEE International Conference on Communications (ICC)**. [S.l.: s.n.], 2011. p. 1–5.

____. Multiuser cooperative diversity through network coding based on classical coding theory. **IEEE Transactions on Signal Processing**, v. 60, n. 2, p. 916–926, 2012.

RIOS, M. et al. Linearity characterization of a CMOS power amplifier for IEEE 802.15.4, IEEE 802.11n and LTE signals. In: **XXII Iberchip Workshop**. [S.l.: s.n.], 2016.

ROSAS, F.; OBERLI, C. Modulation and SNR optimization for achieving energy-efficient communications over short-range fading channels. **IEEE Transactions on Wireless Communications**, v. 11, n. 12, p. 4286–4295, 2012.

RUIZ, H. S.; PÉREZ, R. B. Impact of PA on integrated transceivers. In: **Linear CMOS RF Power Amplifiers: A Complete Design Workflow**. 1st ed.. ed. [S.l.]: Springer, 2014.

SALIM, M. M. et al. Optimal resource and power allocation with relay selection for RF/RE energy harvesting relay-aided D2D communication. **IEEE Access**, v. 7, p. 89670–89686, 2019.

SANTOS, E. L.; LEITE, B.; MARIANO, A. Multimode 2.4 GHz CMOS power amplifier with gain control for efficiency enhancement at power backoff. In: **IEEE 6th Latin American Symposium on Circuits Systems (LASCAS)**. [S.l.: s.n.], 2015. p. 1–4.

SANTOS, E. L. et al. A fully integrated CMOS power amplifier with discrete gain control for efficiency enhancement. **Microelectronics Journal**, v. 70, p. 34–42, 2017. ISSN 0026-2692.

SANTOS, E. L. D. et al. Energy efficiency in multiple antenna machine-type communications with reconfigurable RF transceivers. **IEEE Access**, v. 7, p. 113031–113042, 2019.

SANTOS, E. L. dos et al. Energy analysis in cooperative machine-type communications with reconfigurable RF transceivers. In: **XXXVIII Simpósio Brasileiro de Telecomunicações e Processamento de Sinais (SBrT 2020)**. [S.l.: s.n.], 2020.

SANTOS, F.; MARIANO, A.; LEITE, B. 2.4 GHz CMOS digitally programmable power amplifier for power back-off operation. In: **2016 IEEE 7th Latin American Symposium on Circuits Systems (LASCAS)**. [S.l.: s.n.], 2016. p. 159–162.

SANTOS, F. G.; LEITE, B. R. B. de A.; MARIANO, A. A. A novel single propagation path multimode PA. In: **2020 33rd Symposium on Integrated Circuits and Systems Design (SBCCI)**. [S.l.: s.n.], 2020. p. 1–6.

SENDONARIS, A.; ERKIP, E.; AAZHANG, B. User cooperation diversity: Part I and Part II. **IEEE Transactions on Communications**, v. 51, n. 11, p. 1927–1948, 2003.

SILJAK, H.; PSARA, K.; PHILIPPOU, A. Distributed antenna selection for massive MIMO using reversing petri nets. **IEEE Wireless Communications Letters**, v. 8, n. 5, p. 1427–1430, 2019.

SIMON, M. K.; ALOUINI, M.-S. Digital communications over fading channels (m.k. simon and m.s. alouini; 2005) [book review]. **IEEE Transactions on Information Theory**, v. 54, n. 7, p. 3369–3370, 2008.

SOUZA, M. D.; MARIANO, A.; TARIS, T. Reconfigurable inductorless wideband CMOS LNA for wireless communications. **IEEE Transactions on Circuits and Systems I: Regular Papers**, v. 64, n. 3, p. 675–685, 2017.

STEER, M. **Microwave and RF Design: A Systems Approach**. 1st. ed. [S.l.]: SciTech Publishing, 2010.

SUN, Z. et al. A 0.85mm2 BLE transceiver using an on-chip harmonic-suppressed RFIO circuitry with T/R switch. **IEEE Transactions on Circuits and Systems I: Regular Papers**, v. 68, n. 1, p. 196–209, 2021.

TARUI, B. Y. et al. Design of an RF six-mode CMOS power amplifier for efficiency improvement at power backoff. In: **31st Symposium on Integrated Circuits and Systems Design (SBCCI)**. [S.l.: s.n.], 2018.

TEXAS INSTRUMENTS. **CC13xx Antenna Diversity. Application Report SWRA523B**. [S.l.], March 2017. Available in: <www.ti.com/lit/an/swra523b/swra523b-.pdf?ts=1611754045443&ref_url=https%253A%252F%252Fwww.google.com%252F>.

TSE, D.; VISWANATH, P. **Fundamentals of Wireless Communication**. [S.l.]: Cambridge University Press, 2005. ISBN 9780521845274.

TUAN, N. T.; KIM, D.; LEE, J. On the performance of cooperative transmission schemes in industrial wireless sensor networks. **IEEE Transactions on Industrial Informatics**, v. 14, n. 9, p. 4007–4018, 2018.

U.S. DEPARTMENT OF ENERGY. **Energy Storage Grand Challenge: Energy Storage Market Report**. [S.l.], December 2020. Available in: <www.energy.gov/sites/prod/files/2020-/12/f81/Energy%20Storage%20Market%20Report%202020_0.pdf>.

WANG, X.; ASHIKHMIN, A.; WANG, X. Wirelessly powered cell-free IoT: Analysis and optimization. **IEEE Internet of Things Journal**, v. 7, n. 9, p. 8384–8396, 2020.

WANG, Y.; HUANG, Z.; JIN, T. A 2.35/2.4/2.45/2.55 GHz low-noise amplifier design using body self-biasing technique for ISM and LTE band application. **IEEE Access**, v. 7, p. 183761–183769, 2019.

XIA, N.; CHEN, H. H.; YANG, C. S. Emerging technologies for machine-type communication networks. **IEEE Network**, v. 34, n. 1, p. 214–222, 2020.

XIAO, M.; SKOGLUND, M. M-user cooperative wireless communications based on nonbinary network codes. In: **2009 IEEE Information Theory Workshop on Networking and Information Theory**. [S.l.: s.n.], 2009. p. 316–320.

YABCZNSKI, E. et al. Energy efficient probabilistic switching on?off operation in multiantenna cooperative wireless sensor networks. **Sensors**, v. 21, n. 9, 2021. ISSN 1424-8220. Available in: <https://www.mdpi.com/1424-8220/21/9/2937>.

YANG, P. et al. Adaptive spatial modulation mimo based on machine learning. **IEEE Journal on Selected Areas in Communications**, v. 37, n. 9, p. 2117–2131, 2019.

YOO, T.; JINDAL, N.; GOLDSMITH, A. Multi-antenna downlink channels with limited feedback and user selection. **IEEE Journal on Selected Areas in Communications**, v. 25, n. 7, p. 1478–1491, 2007.

YU, X. et al. Power allocation for energy efficient optimization of distributed MIMO system with beamforming. **IEEE Transactions on Vehicular Technology**, v. 68, n. 9, p. 8966–8981, 2019.

ZAINI-DESEVEDAVY, J. et al. An ultra-low power 28 nm FD-SOI low noise amplifier based on channel aware receiver system analysis. **Journal of Low Power Electronics and Applications**, v. 8, n. 2, 2018. ISSN 2079-9268.

ZAINI, J. et al. A tunable ultra low power inductorless low noise amplifier exploiting body biasing of 28 nm FDSOI technology. In: **IEEE/ACM International Symposium on Low Power Electronics and Design (ISLPED)**. [S.l.: s.n.], 2017. p. 1–6.

ZHAO, M. et al. Joint transmit beamforming and antenna selection in MIMO systems. **IEEE Wireless Communications Letters**, v. 7, n. 5, p. 716–719, 2018.

ZHU, W.; ZHANG, L.; WANG, Y. A 10.56-GHz broadband transceiver with integrated T/R switching via matching network reuse and 0.3?2.1-GHz baseband in 28-nm CMOS technology. **IEEE Transactions on Microwave Theory and Techniques**, v. 67, n. 7, p. 2599–2617, 2019.

ZOU, Y.; ZHU, J.; JIANG, X. Joint power splitting and relay selection in energy-harvesting communications for IoT networks. **IEEE Internet of Things Journal**, v. 7, n. 1, p. 584–597, 2020.